MATERIALS CHEMISTRY FRONTIERS

REVIEW

View Article Online
View Journal | View Issue

Cite this: *Mater. Chem. Front.*, 2021, **5**, 6735

Recent advances in bone-targeting nanoparticles for biomedical applications

Xue Zhou,[a] Erik Jan Cornel,[a] Shisheng He*[b] and Jianzhong Du *[ab]

Received 10th June 2021,
Accepted 14th July 2021

DOI: 10.1039/d1qm00851j

rsc.li/frontiers-materials

As the hardest connective tissue, bone tissue is an important part of the human body. However, with the increasing average age of the global population, the incidence of bone-related diseases has increased significantly. In view of the limitations of clinical diagnosis and treatment of bone-related diseases, nanomaterials that can be applied to bone-related diseases have attracted extensive attention. Among them, nanoparticles with the ability to specifically target bone tissues have become a research hotspot. Herein, we review advances in bone-targeting nanoparticles. First, we classify the most common bone-targeting functional groups and discuss the corresponding bone-targeting mechanisms. Then, we enumerate the existing types of bone-targeting nanoparticles and outline the latest research progress. Finally, we summarize the applications of bone-targeting nanoparticles for the treatment of cancer and osteoporosis, and for the diagnosis of bone-related diseases. This review uncovers the potential use of bone-targeting nanoparticles for the diagnosis and treatment of bone-related diseases and provides guidance for future research in this field.

1. Introduction

Bone tissue is composed of bone cells that are confined within the bone matrix. Bone cells, including osteoblasts, osteoclasts, and osteocytes, work together to complete bone resorption and remodeling, and to maintain the dynamic bone metabolism balance. The bone matrix is composed of an organic substance and highly mineralized hydroxyapatite (HA) crystals. The organic part occupies ~22% and the inorganic part fills up ~65-to-75% of dry bone weight.[1] The organic part is mainly composed of collagen fibrils, proteoglycans, and lipids; collagen fibrils occupy more than 90% of the total organic weight. The inorganic part is mainly composed of calcium, phosphorus, and magnesium. Inorganic amorphous calcium and phosphorus can be found in the form of HA crystals within the organic bone material. Most of the calcium in the human body

[a] *Department of Polymeric Materials, School of Materials Science and Engineering, Tongji University, 4800 Caoan Road, Shanghai 201804, China. E-mail: jzdu@tongji.edu.cn*
[b] *Department of Orthopedics, Shanghai Institute of Bone Tumor, Shanghai Tenth People's Hospital, Tongji University, Shanghai 200072, China*

Xue Zhou

Xue Zhou obtained her BS degree in Materials Science and Engineering from Fuzhou University in 2016. She is currently a PhD candidate at Tongji University under the supervision of Prof. Jianzhong Du. Her research focuses on the design, synthesis and application of bone-targeting polymer vesicles.

Erik Jan Cornel

Erik J. Cornel obtained his master's degree in 2015 and PhD degree in 2019 at the University of Sheffield (UK) under supervision of Prof. Steven P. Armes. His projects involved the preparation of nanoparticles via Polymerization-Induced Self-Assembly (PISA) and the characterization of block copolymer chain exchange between such nanoparticles using SAXS and SANS. Currently, since 2020, he is working in Shanghai (China) at Tongji University with Prof. Jianzhong Du. His projects involve the efficient synthesis of biodegradable nanoparticles using PISA.

(99%) is present within the bone tissue. This tissue is the main source of inorganic ions in the body and it maintains the homeostatic state of calcium and phosphorus.[2] Bone tissue is a dense and hard material owing to the large amounts of calcium salts deposited into the intercellular stroma. However, bone tissue is not present in a rigid state as it constantly undergoes a self-renewing progress. In other words, it constantly balances absorption and reconstruction. Breaking this balance, by external or internal factors, leads to the occurrence of bone diseases.

Bone diseases include osteoporosis, primary malignant bone tumor, bone metastasis, osteoarthritis, osteopetrosis, bone pain, *etc.* Osteoporosis is one of the most common bone diseases with a high incidence in the elderly population, especially in postmenopausal women.[3,4] Statistics show that about 40% of the patients with osteoporosis suffer from bone fracture, and, once occurred, the patient will face serious complications and might even die during treatment. Primary malignant bone tumors as well as bone metastasis have a high mortality rate. Osteosarcoma is one of the most common primary malignant bone tumors and is the eighth most common cancer occurring in adolescents.[5] Bone metastasis is the typical late-stage cancer symptom; more than 70% of the patients that die from cancer suffer from this complication.[6] Bone metastasis can lead to a series of bone-related complications, including bone pain, osteoarthritis, bone loss, fracture, *etc.* On average, these complications occur every 3–6 months and can cause a serious threat to patients' lives.[7] However, there are many limitations in the clinical treatment of these bone-related diseases, leading to unsatisfactory therapeutic outcomes.[8–11]

The application of nanomaterials in the biomedical field has attracted a tremendous amount of attention because of their advantages.[12–14] They have brought huge advantages for the diagnosis and treatment of various diseases: (1) unlike the conventional systematic drug administration approach, nanoparticles can be functionalized with targeting groups to achieve targeted drug delivery. This can increase the local drug concentration, hence improving the therapeutic efficiency while avoiding undesired side effects to healthy tissues. (2) Nanoparticles can protect the loaded drugs from the biochemical environment in the body, leading to a prolonged drug activity. (3) Nanoparticles can load hydrophobic drugs; here nanoparticles can greatly promote the efficiency of such water-insoluble compounds. (4) Drug-loaded nanoparticles have better stability in the body compared to small molecule drugs, which can therefore increase the drug circulation time, allowing a reduced drug administration frequency. (5) Nanoparticles can be designed with multiple therapeutic functions. For example, one kind of nanoparticle can be used for diagnosis and treatment.

Nanoparticles can be designed with the ability to target bone tissue. Additional functions can be achieved by chemical modification and drug encapsulation (Scheme 1). Functionalized bone-targeting nanoparticles have great application value for the diagnosis and treatment of bone-related diseases.[15–17]

Generally speaking, the surface of bone-targeting nanoparticles consists of bone-targeting ligands, which directs these nanomaterials towards the bone tissue. The general concept of bone targeting was proposed by Pierce *et al.* in 1986.[18] Bone targeting ligands can specifically bind the HA in the bone tissue. However, nanoparticles have gradually become more sophisticated as they can target the osteocytes or the organic part of the bone.

Commonly used bone-targeting ligands include bisphosphonates, tetracycline, polypeptides, and small molecular heterocycles.[16] Bisphosphonates are the most widely used bone-targeting ligands.[19] Currently, there are three generations of bisphosphonates approved for clinical use and are mainly used for the treatment of osteitis deformans, osteoporosis, bone defects, and bone metastasis.[20] However, it is worth noting that bisphosphonates have some undesired side effects and could remain within the bone tissue for a long time.

Shisheng He

Shisheng He is a Professor and Director of the Department of Orthopedics, Shanghai Tenth People's Hospital, Tongji University. He is an expert in minimally invasive spinal surgery and has done a lot of work in minimally invasive spinal surgery, instrument design, doctor training and scientific research.

Jianzhong Du

Prof. Jianzhong Du FRSC received his PhD degree in chemistry in 2004 from the Institute of Chemistry, CAS. Then he worked at Sheffield University (2004–2005, 2006–2008), Cambridge University and Warwick University (2008–2010) as a postdoctoral fellow, and at TU-Chemnitz (2005–2006) as an Alexander von Humboldt fellow. He was appointed as an 'Eastern Scholar' professor in 2009. Currently, he is the head of department of polymeric materials at Tongji University, and the recipient of the National Science Fund for Distinguished Young Scholars. His research focuses on polymer synthesis and polymer vesicles for biomedical applications.

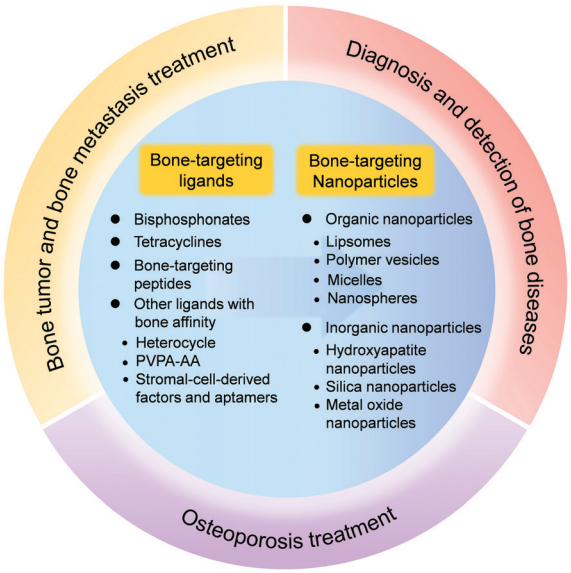

Scheme 1 Schematic illustration of the categories and applications of bone-targeting nanoparticles.

Indeed, the long-term use of bisphosphonates may cause necrosis of the jaw and fracture of the femur.[21] Various studies have also been conducted where peptides are used as bone-targeting ligands. Such peptides have better biocompatibility than bisphosphonates; however, they exhibit a weaker bone affinity.[22] Additionally, small molecule heterocycles, osteocyte targeting ligands [selected by Systematic Evolution of Ligands by Exponential Enrichment (SELEX)], and tetracyclines can also be used as bone-targeting ligands.[23–26]

Bone-targeting nanoparticles can be constructed from lipids, polymers, polypeptides, silica, metal oxides, *etc.*[27] Such nanoparticles can also be classified based on their morphology as follows: polymer vesicles or micelles, liposomes, solid nanospheres and core–shell nanospheres.[16] Some of these nanoparticles show inherent affinity for bone tissue, and here bone-targeting ligands are not required. Examples of such materials are HA nanoparticles, titanium dioxide nanoparticles, and rare earth doped nanoparticles.[28–30] These kinds of nanoparticles are widely used in bone tissue engineering and bone imaging.

In this review, we present the advances in the design and biomedical applications of bone-targeting nanoparticles. First, we summarize the commonly used bone-targeting ligands and explain their bone targeting mechanism. Subsequently, various different bone-targeting nanoparticles are discussed and representative examples are highlighted. Finally, we provide an overview of bone-targeting nanoparticles for the diagnosis and treatment of specific bone diseases.

2. Bone-targeting ligands

2.1 Bisphosphonates

Exploration of the physiological action of pyrophosphate began in the 1960s.[31] Pyrophosphate is a natural compound distributed on the surface of bone HA crystals, and its function is related to the formation and dissolution of HA crystals *in vivo*.[32] The molecular structure of pyrophosphate is shown in Fig. 1, which is composed of one oxygen atom that connects two phosphate groups. The P–O–P bond in pyrophosphate can be easily hydrolyzed *in vivo* by enzymes, which leads to the loss of its bone-targeting ability. Therefore, pyrophosphate is not a suitable bone-targeting ligand and bisphosphonates are further studied as synthetic analogues.

Compared to pyrophosphate, bisphosphonates exhibit superior *in vivo* stability, owing to the P–C–P bond.[33] This bond angle is close to the angle of the two separated oxygen atoms in HA. Therefore, bisphosphonates have the affinity to bind to bone tissue.[34,35] In addition to the two phosphate groups, there are two additional side groups (R_1, R_2) that are connected to the carbon atom of bisphosphonates.[19] Bisphosphonates do not only have special affinity for bone tissue, but these compounds also offer certain beneficial pharmacological effects that can inhibit bone resorption and the development of bone tumors.[36–38] The spatial configuration of bisphosphonates and the structures of the R_1 and R_2 groups both have an impact on

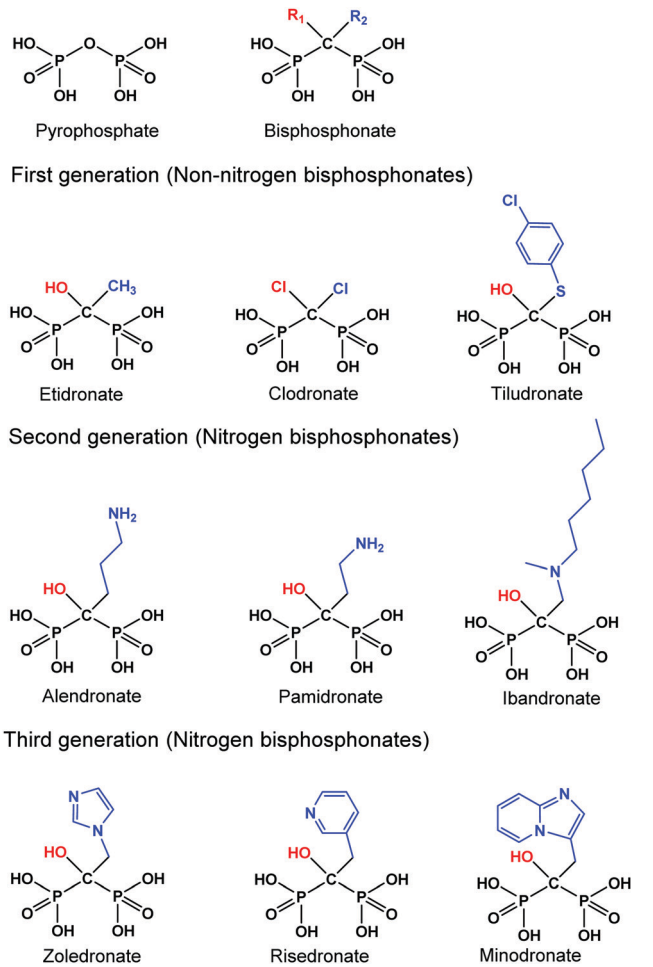

Fig. 1 Structure of pyrophosphate and bisphosphonates. The difference of bisphosphonates mainly depends on the structures of R_1 and R_2 groups, and they are divided into three generations.

the bone-targeting ability and the biological activity of bisphosphonates.[39–41]

There are three generations of bisphosphonates approved for clinical use:[19,20] (1) the first generation includes etidronate, chlorophosphonate, and sodium tiludronate. The R_2 groups of these bisphosphonates are relatively small and their bone resorption inhibition ability is weak. (2) The second generation consists of alendronate, pamidronate, ibandronate, *etc.* These groups show a stronger bone affinity than the first generation. (3) The third comprises zoledronic acid, risedronic acid, aminophosphonic acid, *etc.* The anti-resorption ability of this generation is significantly increased because of the introduction of heterocyclic aromatic group in the R_2 group.[42] In terms of chemical structure, the first generation are nitrogen-free bisphosphonates, and the second and third generations are nitrogen-containing bisphosphonates.

The specific binding of bisphosphonates to bone tissue is mainly through ion exchange and chemical adsorption. First, the bone affinity of bisphosphonates is affected by the spatial configuration and the R_1 group.[43] For example, olpadronate and etidronate have a similar spatial configuration and a hydroxyl group (–OH) at the R_1 site. These two bisphosphonates can replace dimethyl-pamidronate from mouse fetal bones with a similar efficacy, while that of clodronate (with no R_1 group) is much lower.[39] This is related to the different way that bisphosphonates bind HA. The deprotonated oxygen ions ($-O^-$) of the two phosphate groups from the bisphosphonates and the Ca^{2+} in HA will form a bidentate binding in the absence of a R_1 group. Here, a tridentate binding will be formed with –OH at the R_1 site.[44] Secondly, the R_2 group also has an influence on its bone compatibility.[45,46] Bisphosphonates with a nitrogen-containing R_2 group will show a higher bone affinity than nitrogen-free bisphosphonates.[47] This is caused by the different protonation of R_2 groups, which leads to a different surface charge of the HA and subsequently affects the binding process.[47] Besides, some nitrogen-containing bisphosphonates can form hydrogen bonds with HA, which further enhances the binding force.[48,49] The hydrophilicity of bisphosphonates also affects their bone affinity. Studies have shown that the hydrophilicity of the metal chelation of bisphosphonates is related to its inherent hydrophobicity. Metal chelation of bisphosphonates with poor hydrophilicity will be removed faster *in vivo*, and this is not conducive to the binding process. Therefore, hydrophilic bisphosphonates have a greater bone affinity.[50]

In addition to the bone-targeting ability, bisphosphonates were also clinically used for the inhibition of bone resorption and tumor growth (Table 1).[51,52] The pharmacokinetics of bisphosphonates were mainly decided by the R_2 group.[45] For bone resorption inhibition, nitrogen-containing bisphosphonates can disturb the biological metabolism of osteoclasts leading to osteoclast apoptosis. Additionally, nitrogen-free bisphosphonates can hinder the synthesis of proteins and other substances that are necessary for bone absorption.[53] The tumor growth inhibition can be achieved by both direct and indirect ways: bisphosphonates can directly inhibit the adhesion and invasion of the tumor to bone tissue,[54] and these compounds can indirectly prevent angiogenesis and activate the immune tissue.[19,21,55,56] Additionally, the anti-resorption ability of bisphosphonates can also inhibit malignant osteolysis caused by tumors. However, large doses of bisphosphonates can lead to undesired side effects, such as gastrointestinal irritation, necrosis of the jaw, renal damage, esophageal cancer, and atypical fracture.[57–59] By binding bisphosphonates to nanoparticles, better therapeutic effects can be achieved with a lower required dose, thus avoiding side effects to some extent.

2.2 Tetracyclines

The earliest studies on tetracyclines were based on their broad spectrum of antibiotic activity against Gram-positive bacteria, Gram-negative bacteria, protozoan parasites, *etc.* and are nowadays a widely used class of antibiotics.[60–63] The general molecular structure of tetracyclines consists of four linear-linked six-membered rings with different functional groups (Fig. 2).[60,64] According to different sources, tetracyclines can be divided into natural tetracyclines (tetracycline, chlortetracycline, oxytetracycline, *etc.*) and semi-synthetic tetracyclines (methacycline, rolitetracycline, *etc.*). Additionally, chemically modified tetracyclines (CMTs) are also commonly used.[23,65]

The bone-targeting ability of tetracyclines was discovered in the 1960s. Tetracycline depositions can be detected by fluorescence microscopy of the bone without decalcification.[66,67] Compared to alizarin red and heavy metal markers, tetracyclines are much safer and the labelling process is more convenient. For these reasons, tetracyclines were commonly used as fluorescent markers to observe the formation and pathological changes of the bone.[68–70] It was initially hypothesized that tetracyclines interact with the organic part of the bone tissue.[71] Later studies reported that they have the ability to chelate with calcium and to bind HA on the bone surface.[72]

Table 1 Summary of bone-targeting ligands

Bone-targeting ligand	Advantages	Disadvantages	Clinical use
Bisphosphonates	Strong bone affinity and long retention time	Undesired side effects caused by long-term use	Treatment of osteoporosis, inhibition of tumor growth and malignant osteolysis
Tetracyclines	Inherent antibacterial and fluorescence properties, high affinity to bone with high turn-over	Low affinity to pathologic bone sites with low bone turn-over	Fluorescent bone markers and antibiotics
Bone-targeting peptides	Adjustable bone-targeting ability, good biocompatibility and biodegradability	Relatively low stability and prone to hydrolysis and loss efficacy	—

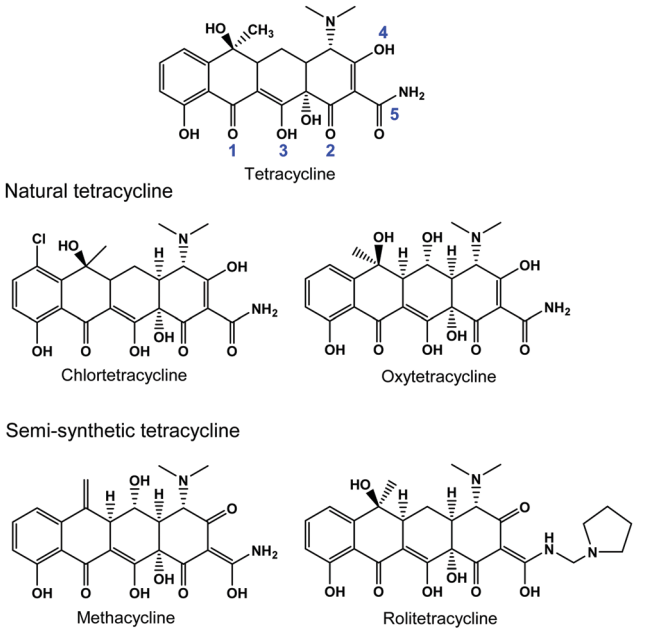

Fig. 2 The chemical structures of tetracyclines. The β-carbonyl groups at sites 1 and 2, the hydroxyl groups at sites 3 and 4, and the carboxamide group at site 5 are responsible for the HA binding capacity of tetracyclines.

In terms of the molecular mechanism, the β-carbonyl groups at sites 1 and 2, the hydroxyl groups at sites 3 and 4, and the carboxamide group at site 5 (as shown in Fig. 2) are responsible for the HA binding capacity of tetracyclines.[73,74]

Tetracyclines also play a role in bone metabolism. Tetracyclines can inhibit bone resorption by affecting the metabolism of osteoclasts:[65,75,76] first, tetracyclines can inhibit the activity of osteoclast matrix metalloproteinase (MMP), collagenase, gelatinase, and cysteine proteinase, which play a key role in the formation and activity of osteoclasts. Secondly, tetracyclines can narrow the hair-like protuberant area of the osteoclast, through which the osteoclast can bind to the surface of the bone and dissolve the bone matrix. Thirdly, tetracyclines can remove reactive oxygen species that can activate MMP within the extracellular matrix. However, the effects of tetracyclines on the metabolism of osteoblasts are concentration-dependent: low tetracycline concentrations can induce osteoblast proliferation and promote bone mineralization; on the contrary, high concentrations inhibit the proliferation process.[77,78] Therefore, the dosage of tetracyclines is of importance. Besides, since it has been reported that cancer bone metastasis and tumor cell-mediated osteolysis are mediated by MMP,[79–81] tetracyclines also display potential antitumor activity by inhibiting the activity of MMP and antiangiogenesis (Table 1).[82–84]

2.3 Bone-targeting peptides

Non-collagen bone proteins such as osteocalcin,[85] osteopontin,[86] and bone sialoprotein,[87] as well as proteins existing in human saliva and teeth such as proline acidic protein and dentin phosphoprotein, have affinity for bone tissue and play an important role in the nucleation, growth, and dissolution of bone apatite.[88,89] These natural proteins in the human body are a source of inspiration for the design and synthesis of bone-targeting peptides.

It is found that the repeating sequences of glutamate (Glu) and aspartate (Asp) in osteopontin and sialoprotein play a key role in bone affinity. Therefore, these sequences were used for bone-targeting applications. In 1991, Fujusawa *et al.* found that short peptides composed of Glu or Asp repeat units would preferentially adsorb on the (100) surface of HA crystals.[90] In 2000, Kasugai *et al.* demonstrated the good bone-targeting ability and potential of a FITC-labelled hexapeptide chain $(Asp)_6$ for applications in bone-targeting drug delivery systems.[91] Later, Miyamoto *et al.* compared the HA affinity of a series of Glu and Asp peptides with different chain lengths and peptide conformations. In this study, they found that the bone affinity of these peptides was mainly influenced by the number of repeat units, but not the kind of the evaluated amino acid. More specifically, the HA binding ability increased when the number of Glu or Asp repeat units increased from 2 to 10.[22] Masayuki *et al.* found that α-aspartic peptides exhibit a stronger binding force towards calcium ions than both β-aspartic peptides and α,β-aspartic peptides. This indicates that the bone affinity of bone-targeting peptides is also affected by the type of peptide bond.[92]

The *in vivo* stability of bone-targeting ligands also plays an important role. The peptide stability is related to their chiral conformation. It was found that the L-Asp_6 peptides broke down rapidly in the bloodstream, whereas the D-Asp_6 remained stable for a relatively long time. The is because chirality can affect the solubility: D-Asp_6 is more hydrophobic than L-Asp_6.[22] However, biodegradability is affected by neither the chirality nor the type of peptide bond.[92]

In addition to the above two types of peptides, other peptides that show bone affinity have been studied. Bennick *et al.* analyzed salivary acidic proline-rich proteins and found that the phosphoserine (Ser) plays an important role in its affinity to HA.[93] Yarbrough *et al.* studied dentin phosphoprotein and found that the tripeptide Asp-Ser-Ser and its repeating sequences had affinity for the mineralized surface of bones.[94] Further studies showed that different kinds of peptides can selectively bind to different bone surfaces.[95] Asp_8 is more likely to target the bone resorption surface,[96] while $(Asp\text{-}Ser\text{-}Ser)_6$ is more likely to bind to the bone formation surface.[97] Qin *et al.* demonstrated that this is caused by differences in the degree of crystallization of HA on the bone surface: the bone formation surface dominated by osteoblasts is covered with HA with a low crystallization degree; the bone resorption surface dominated by osteoclasts is covered with HA with a high crystallization degree.[96] Through the analysis of amino acid sequences in natural proteins, more peptides with bone affinity can be found and applied in bone-targeting nanoparticles. The development of bone-targeting artificial osteophilic polypeptides with adjustable targeting or special recognition has potential research value (Table 1).[98]

Peptides that can target bone cells have been established with the development of analytical methods, such as phage

display technology, enzyme-linked immunosorbent assay (ELISA), and computer simulation. For example, Wang *et al.* examined the affinity of the bone formation surface for Ser-Asp-Ser-Ser-Asp peptides using phage display technology and subsequently used this sequence for RNA delivery.[99] Kohn *et al.* elucidated three peptides with high affinity for bone apatite: APWHLSSQYSRT [A], STLPIPHEFSRE [S], and VTKHLNQISQsy [VTK] by a combination of phage display, ELISA, and computational modeling.[100] More specifically, they analyzed the effects of phosphorylation, morphology and composition of amino acids on the bone affinity of these peptides. Phosphorylation can improve the bone affinity of these peptides, which can reduce the isoelectric point of peptides and increase their negative charge, thus facilitating the interactions between polypeptides and calcium in HA.[101] On this basis, Sahai *et al.* systematically studied the effects of primary amino acid sequence, phosphorylation, the charge density of peptide side chains, and the magnitude of the net charge on the bone affinity of bone-targeting peptides. Here, it was found that the magnitude of the net charge is the major factor that influences the bone affinity of peptides.[102]

2.4 Other ligands with bone affinity

Apart from bisphosphonates, tetracycline, and peptides, other kinds of potential bone-targeting ligands have been evaluated as well: Willson *et al.* synthesized a series of small heterocycles based on the chemical structure of thiadiazole and found that these small heterocycles exhibited bone-targeting properties. Among them, 4-carboxy-3-hydroxy-l,2-pyrazole exhibited similar bone-affinity to tetracycline.[24] Zakikhani *et al.* found that the phosphonate-containing ionic polymer poly(vinyl phosphonic acid-*co*-acrylic acid) (PVPA–AA) has similar functions and bone-targeting properties to bisphosphonates. They hypothesized that this resemblance is on one hand related to the P–C bond of PVPA–AA, since this is similar to the P–C–P bond in bisphosphonates; on the other hand, it was suggested that the negative charge of PVPA–AA gives PVPA–AA a strong ability to bind calcium ions.[103] Additional research suggested that the bone affinity of PVPA–AA was similar to that of alendronic acid, nitrogen-free clodronate, and etidronate.[104] Cabasso *et al.* found that phosphorylated poly(*p*-phenylene oxide) has bone affinity. They found that semi-acids and semi-esters can rapidly be adsorbed on HA; the rate and amount of adsorption are positively correlated with the concentration. Additionally, non-ionic polymers such as chitosan, glucan, and *N*-methacrylamido salicylic acid also have bone targeting properties.[95,98]

In addition to chemical compounds, stromal-cell-derived factor and aptamers have also been used as targeting groups: for example, Zhang *et al.* screened the osteoblast-specific aptamer CH6 ligand using cell-SELEX for the delivery of short interfering RNA (siRNA);[25] Dai *et al.* found that that collagen-binding stromal-cell-derived factor-1α (CBD-SDF-1α) can strongly bind to mesenchymal stem cells and promote bone regeneration.[26]

3. Bone-targeting nanoparticles

3.1 Organic nanoparticles

3.1.1 Liposomes and polymer vesicles. Liposomes are artificial vesicles made up of natural phospholipids and cholesterol. Phospholipid layers are amphiphilic in aqueous solution, wherein the hydrophobic lipid layers will form a closed spherical membrane driven by an increase in thermodynamic entropy. During this process the hydrophilic parts extend inside and outside while forming the membrane.[105] The size of such liposomes ranges from 25 nm to 2.5 μm. Single layer liposomes tend to possess a single hydrophilic lumen, while multilayer liposomes possess an onion-like structure with multiple lumens.[106] Properties of liposomes vary greatly with their size, surface charge, composition, and preparation method.[107] Liposomes have great potential for biomedical applications. Liposomes composed of natural phospholipids have superior biocompatibility and biodegradability compared with other nanoparticles. As a drug carrier, liposomes can protect drugs from enzymes and the body's immune system. Additionally, such drug vehicles deliver drugs to a targeted location, thus not only reducing the side effects of drugs, but also improving the drug efficacy.[108] Both hydrophilic and hydrophobic drugs can be encapsulated in liposomes, but the drug locations are different: hydrophobic drugs are mainly loaded within the hydrophobic membrane, while hydrophilic drugs are mainly encapsulated in the hydrophilic cavities.[109] Liposomes are mainly prepared with two methods: the mechanical dispersion method and the solvent dispersion method. The mechanical dispersion method involves sonication, extrusion, freezing–thawing, mechanical shaking, micro-emulsion, or membrane extrusion. The solution dispersion method is mainly based on solvent evaporation, ether injection, reverse phase evaporation, lyophilization/rehydration, *etc.*[110] Bone-targeting ligands can be chemically grafted to polymer chains before the liposome assembly or be incorporated post-preparation on the surface of the liposomes to make them suitable for the diagnosis and treatment of bone diseases.

Zhang *et al.* prepared dioleoyl trimethylammonium propane (DOTAP)-based cationic liposomes using the lyophilization/rehydration method and modified these liposomes with $(Asp-Ser-Ser)_6$ to realize the bone-targeted delivery of the osteogenic siRNA Plekho1.[97] *In vivo* drug distribution experiments showed that the Plekho1 delivered by these functionalized liposomes had the highest aggregation concentration in bones compared with unmodified liposomes or the direct injection approach. Additionally, the distribution of the siRNA Plekho1 in non-skeletal tissues was significantly reduced. Moreover, it was also found that these functionalized liposomes were more likely to bind to the bone formation surface rather than the bone resorption surface. It was speculated that the ability to specifically target the bone formation surface promotes the siRNA Plekho1 mediated Plekho1 gene silence and, therefore, significantly increases the life span and activity of osteoblasts.

Katsumi *et al.* developed a polyethylene glycol (PEG)-conjugated aspartic acid (Asp)-modified liposome (PEG-Asp-Lipo)

as a bone-targeting carrier of paclitaxel (PTX). Here, these liposomes were co-assembled with Asp-modified 1,2-dipalmitoyl-*sn-glycero*-3-phosphoethanolamine (DPPE-Asp) and *N*-(carbonyl-methoxypolyethyleneglycol 2000)-1,2-distearoyl-*sn-glycero*-3-phosphoethanolamine, sodium salt (DSPE-PEG).[111] They found that the affinity of PEG-Asp-Lipo to the bone increased with the proportion of the DPPE-Asp. It was hypothesized that Asp could chelate with the calcium ions of the bone tissue, thus increasing the bone affinity, and that the adsorption of PEG-Asp-Lipo to HAP was sterically prevented by the relatively large PEG molecules, thus reducing the bone affinity. *In situ* imaging results showed that PEG-Asp-Lipo mainly aggregated in the epiphysis and at the proximity of the joint. It was concluded that PEG-Asp-Lipo was more likely to interact with the epiphysis, which is associated with the pathogenesis of various bone diseases. Subsequently, they found that these liposomes tended to accumulate onto eroded and quiescent surfaces where osteoclasts are active and further induce the apoptosis of osteoclasts (Table 2).

Polymer vesicles consist of multiple aggregated polymer chains. Such polymers have a molecular weight distribution and, in comparison to natural liposomes, a much larger molecular weight. Such features lead to a more stable and robust structure and allow chemical modifications, endowing them with potential for a wide range of biological applications.[112–114] Polymer vesicles are commonly self-assembled from amphiphilic block copolymers. The ratio between the hydrophilic and hydrophobic blocks dictates the final nanoparticle morphology. A ratio between 1 : 2 and 1 : 3 is generally required to form a typical vesicular structure.[115] Critical micellization concentration (CMC) is an important parameter during polymer vesicle formation, which refers to the minimum concentration at which amphiphilic polymers can spontaneously aggregate. Polymer vesicles consist of a hollow spherical morphology with a hydrophobic membrane and hydrophilic inner and outer coronas.[116] The hydrophobic blocks form a closed spherical membrane around a lumen. The hydrophilic blocks stretch on both the inner and outer surfaces of the membrane, forming inner and outer coronas. The lumen of the polymer vesicles can be loaded with hydrophilic guest molecules, such as hydrophilic drugs and bioactive molecules.[115] The hydrophobic membrane can carry hydrophobic guest molecules, such as hydrophobic drugs and dyes. Such an approach can protect the structure and activity of the loaded guest molecules from the external environment.[112,117] The outer coronas can be chemically functionalized to target and image specific tissues and to respond to specific physiological environments.[118]

In addition to the typical hollow spherical structure, polymer vesicles have many other morphologies: bowl shaped vesicles,[119] tetrapod vesicles,[120] elongated tubular vesicles,[121] flower-shaped vesicles,[122] perforated vesicles with a highly folded membrane,[123] *etc.* The vesicular morphology can be affected by many factors, such as the hydrophilic and hydrophobic block ratio of the polymer, the chemical structure of the polymer, concentration in solution, the type of organic solvent, water proportion, pH value, and temperature.[124] There are two general methods for preparing polymer vesicles: the solvent-switch method and the direct hydration method. The solvent-switch method is more widely used, since most amphiphilic block copolymers are not directly soluble in water.[125] However, a disadvantage of this method is that a time-consuming and economically-unfriendly dialysis process is required to remove toxic organic solvents. Additionally, the organic solvent to water ratio has a significant influence on the vesicular morphology, so varying the solvent proportion during the dialysis process impacts the final morphology. To overcome these defects, various new methods have been explored, such as pH-induced self-assembly and polymerization-induced self-assembly.[126–128] The development of these methods provides the possibility of efficient preparation of polymer vesicles.

Polymer vesicles have great potential for the diagnosis and treatment of bone-related diseases. Du *et al.* equipped polymer

Table 2 Summary of bone-targeting nanoparticles

Targeting ligands	Nanoparticle/coating	Cargo	Application	Ref.
$(Asp\text{-}Ser\text{-}Ser)_6$	Liposome	siRNA Plekho1	RNA interference-based bone anabolic therapy	97
Asp	Liposome	Paclitaxel	Treatment of bone metastasis	111
Alendronate	Polymer vesicles	^{99m}Tc/DOX	Diagnosis and treatment of malignant bone tumors	129
Tetracycline	Polymer micelles	Simvastatin	Osteoporosis treatment	137
Alendronate	Polymer micelles	Bortezomib	Treatment of breast cancer bone metastasis	138
Alendronate	PLGA nanoparticles	Curcumin/bortezomib	Treatment of breast cancer bone metastasis	142
Tetracycline	PLGA nanoparticles	Simvastatin	Osteoporosis treatment	143
Risedronate	Chitosan nanoparticles	Risedronate	Osteoporosis treatment	152
—	Gelatin nanoparticles	BMP-2	Growth factor delivery/bone tissue engineering	157
—	Nitrogen-doped carbon dots/nHA	—	Cell imaging/bone regeneration/fracture healing	173
—	Mesoporous nHA	Vincristine	Treatment of bone cancer	174
Zoledronic acid	Gold nanorods/MSNPs	Zoledronic acid	Diagnosis and therapy of bone metastasis	194
Alendronate	MSNPs	Ibuprofen	Bone-specific drug delivery	162
Alendronate	SPION	—	MRI contrast agent	207
Alendronate	Fe_3O_4 nanoparticles	—	Osteoporosis treatment	208
—	TiO_2 NP/collagen/chitosan hydrogels	—	Bone regeneration	211
—	TiO_2 NP/chitosan scaffolds	—	Bone regeneration	212

Asp: aspartic acid, Ser: serine, DOX: doxorubicin hydrochloride, PLGA: poly(lactic-*co*-glycolic acid), BMP-2: bone morphogenetic protein, nHA: hydroxyapatite nanoparticle, MSNP: mesoporous silica nanoparticle, SPION: superparamagnetic iron oxide nanoparticle, MRI: magnetic resonance imaging, NP: nanoparticle.

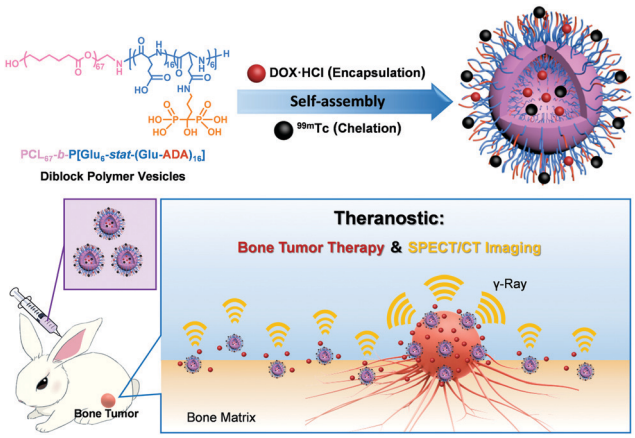

Fig. 3 Schematic illustration of bone-targeting polymer vesicles for simultaneous diagnosis and treatment of malignant bone tumors. Reproduced with permission from ref. 129. Copyright 2021 Elsevier Ltd.

vesicles with the bone-targeting ligand alendronic acid (ADA) for the diagnosis and treatment of malignant bone tumors (Fig. 3).[129] Here, an *in vitro* HA binding experiment showed that the ADA ligands endowed the polymer vesicles with high bone affinity. More specifically, a polymer vesicle was self-assembled from poly(ε-caprolactone)$_{67}$-*b*-poly[(L-glutamic acid)$_6$-*stat*-(L-glutamic acid–alendronic acid)$_{16}$] (PCL_{67}-*b*-P[Glu_6-*stat*-(Glu–ADA)$_{16}$]) directly in water without the aid of an organic solvent. ^{99m}Tc was chelated on the outer coronas to achieve bone imaging and doxorubicin hydrochloride (DOX) was encapsulated in the lumen for tumor therapy. The diameter of this bone-targeting vesicle is 219 nm and has a well-organized morphology and a narrow particle distribution. The DOX encapsulation efficiency is as high as 50.5%. They declared that the electrostatic interactions between the negatively charged corona of the vesicles and the positively charged DOX enabled the hydrophilic lumen to capture this drug more efficiently. Additionally, the bone-targeting polymer vesicles also have pH-responsive drug release capacity, that is, the slightly acidic tumor microenvironment (pH ~ 5) can promote the release of DOX, and 76% of the drug was released from the vesicles in 48 h (Table 2).

3.1.2 Polymer micelles and nanospheres. Dispersed polymer micelles have a 'core–shell' structure and consist of amphiphilic block polymers.[130] These micelles can be assembled in different shapes, such as spherical micelles, rod-like micelles, tubular micelles, sheet-like micelles, *etc.*[131] Micelles with diameters of 20–100 nm are suitable for drug delivery.[132] CMC is also an important parameter in micelle formation. When the polymer concentration reaches the CMC, the hydrophobic block will spontaneously aggregate and form a 'nucleus' and the hydrophilic block acts as a stabilizing 'shell' and provides structural stability. Nanoparticle aggregation is caused by the difference in solubility between the hydrophilic and hydrophobic parts of the amphiphilic polymer in aqueous solution, and the interactions that play a key role include intermolecular (van der Waals), electrostatic, and hydrogen bond interactions.[133]

The hydrophobic micelle core can capture hydrophobic therapeutics, proteins, and genes by chemical or physical binding, and protect these molecular cargoes from a biological environment. The hydrophilic shell of micelles can provide good biocompatibility and increase the circulation time within the body.[134] Additionally, the surface of micelles can be used to modify functional groups that can specifically recognize organs, tissues and cells *in vivo* to achieve targeted drug delivery.[135,136]

Micelles with bone-affinity can be prepared by incorporating bone-targeting ligands on the surface of the micelles. For example, Zou *et al.* modified tetracycline on the amphiphilic copolymer poly(ethylene glycol)-*b*-poly(lactic-*co*-glycolic acid) (PEG-*b*-PLGA) using an amylation reaction. These TC-PEG-PLGA micelles were prepared *via* the solvent diffusion method and the drug simvastatin (SIM) was loaded during the assembly process to obtain the final micelles (TC-PEG-PLGA/SIM).[137] These TC-PEG-PLGA/SIM micelles had a particle size of 56 nm and a CMC of 19.4 μg mL^{-1}, and exhibited good structural stability at both 4 °C and 37 °C. The HA binding rate of TC-PEG-PLGA bone-targeting micelles reached 79% *in vitro* and could effectively aggregate on bone tissue *in vivo*, indicating that TC-PEG-PLGA/SIM micelles had good bone-targeting ability. Additionally, a drug loading efficiency (DLE) of 81.8% was achieved with the TC-PEG-PLGA/SIM micelles; additionally, a continuous *in vitro* drug release for 72 hours was achieved. Both cell and *in vivo* experiments showed that the TC-PEG-PLGA/SIM micelles had no obvious biological toxicity and could significantly prolong the drug circulation time and accumulation in bone tissue.

Niu *et al.* prepared a prodrug micelle (ALN-NP) for combined bone targeting and aryl boronate-based pH-responsive drug release for anti-metastasis therapy.[138] This micelle was co-assembled from two different block copolymers: alendronate-poly(ethylene glycol)-*b*-poly(L-lysine-Z) (ALN-PEG-*b*-PLLZ), for bone-targeting, and PEG-*b*-P(LL-*g*-Cat-BTZ), as the bortezomib drug precursor. The 1,2-benzenediol group (catechol, Cat) was functionalized with bortezomib to form a pH-responsive copolymer that is capable of releasing bortezomib at a low pH. The ALN-NP could effectively cross the blood–bone marrow barrier owing to its nanoscale size and the incorporated ALN groups, therefore promoting the accumulation of these particles in bone metastatic tumor tissues. They found that the bone affinity increased with a larger ALN-PEG-*b*-PLLZ block polymer fraction. The bone affinity did not increase significantly once the content of the bone-targeting ALN-PEG-*b*-PLLZ copolymer in micelles exceeded 20%. *In vivo* experiments showed that ALN-NPs significantly inhibited the growth of breast cancer at bone metastasis sites *in vivo*, and they clearly decreased the degree of bone damage at the bone metastasis sites (Table 2).

According to the composition, organic nanospheres can be divided into poly(lactic-*co*-glycolic acid) nanospheres, chitosan nanospheres, gelatin nanospheres, *etc.*

Poly(lactic-*co*-glycolic acid) nanoparticles (PLGA NPs) are a class of rigid nanoparticles with a solid spherical structure, which are widely used as drug delivery carriers due to their large capacity, good biocompatibility, and adjustable

biodegradation rate.[139] On the one hand, drug release can be regulated by adjusting the lactic-*co*-glycolic acid ratio, particle size, preparation method, *etc.* On the other hand, PLGA NPs can also be functionalized and modified to have diverse functions such as targeting and molecular adsorption.[140] The preparation methods of PLGA NPs can be generally divided into two types: the first type comprises emulsion polymerization, precipitation polymerization, and interfacial polymerization. The second, and the most widely used, method uses pre-formed polymers that are used to prepare nanoparticles through an emulsion diffusion, precipitation, or emulsion evaporation approach.[141]

PLGA NPs also play an important role in bone-targeted drug delivery. Thamake *et al.* prepared alendronate modified PLGA bone-targeting nanoparticles (ALN-PLGA NPs) using a solid/oil/water (s/o/w) emulsion solvent evaporation method for the combined delivery of the anticancer drug curcumin and bortezomib (Fig. 4)[142] using a novel non-covalent chemical crosslinking agent capable of ligand functionalization by carbodiimide chemistry (BS3). This crosslinking agent was inserted into the PLGA polymer, which resulted in the exposure of hydrophilic sulfonic BS3 end-groups on the nanoparticle surface. These activated nanoparticles are prepared in one step and the bone-targeting functionalization could be carried out at physiological pH in an aqueous solution. Here, the thiocyanide group can be removed from BS3, exposing a carboxylic group that is capable of reacting with the amino group in alendronate. The resulting ALN-PLGA NPs are smooth solid spheres with a diameter of 236 nm. The bone affinity of these nanoparticles is three times larger than that of unmodified PLGA NPs. *In vivo* experiments have shown that the ALN-PLGA NPs loaded with curcumin and bortezomib can effectively aggregate in bone tissue, maintain the activity of the two drugs, and release drugs continuously.

Yuan *et al.* synthesized a bone-targeting TC-PLGA polymer using an esterification reaction of the hydroxyl group on tetracycline and the carboxyl group of PLGA. TC-PLGA polymers were used to prepare bone-targeting nanoparticles (TC-PLGA NPs) with the solvent emulsion method. These TC-PLGA NPs were applied for encapsulation and delivery of simvastatin (SIM), an anti-osteoporosis drug.[143] The drug encapsulated nanoparticles (SIM/TC-PLGA NPs) are solid spheres with a diameter of 220 nm which can continuously release 80% SIM for 72 hours. Cell experiments showed that SIM/TC-PLGA NPs could be ingested into MC3T3-E1 cells and significantly reduce the cytotoxicity of SIM. Additionally, *in vivo* experiments showed that TC-PLGA nanoparticles exhibited a significantly increased bone-binding ability compared to untargeted PLGA nanoparticles and effectively reduced drug distribution in other tissues (Table 2).

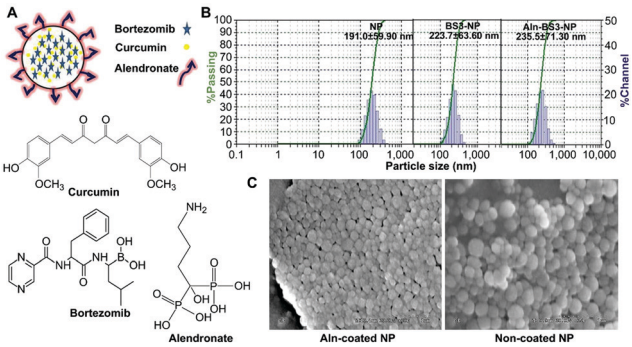

Fig. 4 (A) The schematic diagram of nanoparticles and components of AlN-PLGA NPs. (B) The hydrodynamic particle size of non-activated nanoparticles (without BS3), activated nanoparticles and AlN-PLGA NPs as measured by dynamic light scattering. (C) The hydrodynamic particle size of non-activated nanoparticles (without BS3), activated nanoparticles and AlN-PLGA NPs as measured by dynamic light scattering. Reproduced with permission from ref. 142. Copyright 2012 Elsevier Ltd.

Chitosan and its derivatives are natural polysaccharides formed by the de-acetylation of natural chitin that is composed of varying amounts of glucosamine and *N*-acetyl-glucosamine.[144] Chitosan has good mucosal adhesion, epithelial cell penetration, biocompatibility, biodegradability, and adsorption properties, making it and its derivatives ideal materials for drug delivery carriers.[145–147] Chitosan contains abundant functional groups, such as hydroxyl, amino, acetyl amino, *etc.* The possibility of functionalization of chitosan endows it with diverse chemical properties.[148] Chitosan is insoluble in neutral media, owing to the combined action of the hydrogen bonds and hydrophobic interactions; however, it can be dissolved under slightly acidic conditions.[149] Traditional preparation methods of chitosan nanoparticles include mini-emulsion, chemical or ionic gelation, spray-drying, *etc.* Unfortunately, the cost and the use of a large number of chemical reagents complicate the mass production of chitosan nanoparticles.[150] In recent years, the preparation of chitosan nanoparticles by self-assembly has attracted extensive attention.[151] Santhosh *et al.* prepared risedronate-modified chitosan nanoparticles (RISC NPs) using the ionic gelation technique and used them for the treatment of osteoporosis.[152] The electrostatic interactions of negatively-charged risedronate and positively-charged chitosan, as well as their hydrophobicity, lead to strong interactions between chitosan and risedronate. Meanwhile, cationic chitosan can interact with polyanions to form nanoparticles through inter- and intra-molecular cross-linkages with the addition of alkaline and acidic phases. The SEM results of nanoparticles prepared with this acid–base precipitation method showed that the diameter of the blank chitosan nanospheres was ~110–166 nm and that of RISC NPs was ~175–261 nm. Compared with the blank chitosan nanospheres, the nanoparticle diameter of RISC NPs increased with an increased risedronate proportion. It was hypothesized that the addition of risedronate weakened the molecular interactions between chitosan during the preparation method, leading to larger particle diameters. The risedronate DLE of RISCN NPs was 90 ± 4%; a continuous drug release of 99 ± 3% was achieved after 11 hours.

Gelatin is a natural polymer derived from collagen which has good biocompatibility,[153,154] biodegradability,[155] and non-immunogenicity. This polymer can also easily bind biominerals and biomolecules. Additionally, the electrostatic interactions between the negatively-charged gelatin and the positively-charged protein can achieve controlled and continuous release of proteins from polymer matrices. Therefore, gelatin nanospheres

have great potential for drug and protein delivery.[156] Nanogels formed by cross-linking gelatin nanospheres have adhesive and self-healing properties that can be widely used in bone tissue engineering. Patel *et al.* used gelatin nanoparticles to deliver bone morphogenetic protein (BMP-2).[157] These gelatin nanospheres can release proteins more gradually compared to PLGA NPs. Moreover, acidic conditions can further promote the release of proteins since gelatin nanospheres can be disintegrated at such a pH (Table 2).

3.2 Inorganic nanoparticles

3.2.1 HA nanoparticles. Hydroxyapatite (HA) is the main component of the inorganic part of bone tissue. Nanoparticles prepared from this material are known as nano-HA particles (nHAs). These nHAs can promote bone regeneration and have special biocompatibility/bioactivity towards bone cells and tissues.[158] nHAs are widely used in bone regeneration and bone tissue engineering.[158–162] Presently, the synthesis methods of nHA mainly include electrodeposition, wet chemical deposition, sol–gel, reverse phase microemulsion method, hydrothermal method, microwave irradiation method, *etc.*[163–166] The particle size, surface charge, and other properties have a significant influence on the biological activity of nHAs.

Li *et al.* adjusted the surface charge of a nHA without changing its structure by surface modification with the positively-charged 12-aminododecanoic acid and the negatively-charged dodecanedioic acid, and subsequently studied the cellular uptake behavior and the biological effect on MC3T3-E1 osteoblast cells.[28] They found that untreated, positively-charged, and negatively-charged nHAs with comparable size and properties could penetrate into the cells; however, neutral nHAs with a larger size could not achieve this. More specifically, positively charged nHAs showed a higher cell uptake than negatively charged nHAs. It was hypothesized that the cell uptake is related to the electrostatic attractive/repulsive interaction between the positively/negatively charged nHAs and the negatively charged cell membranes. Besides, compared to non-bioactive polystyrene nanoparticles, all nHAs could enhance the cell viability and cell proliferation. Here, the positively charged nHAs showed the most outstanding performance. Shi *et al.* synthesized nHAs with a diameter of about 20 nm (NP20) and 80 nm (NP80), and micron level rod-like HA (mHA). Afterwards, the effect of the nHA size on the growth and apoptosis of human osteoblast-like MG-63 cells was studied.[167] It was found that the ability of HA particles to promote the proliferation of osteoblasts was negatively correlated with the HA particle size. Compared to mHA, nHA could significantly promote the proliferation of osteoblasts, and the smallest nanoparticles (NP20) showed the highest osteoblast proliferation. They concluded that the larger surface area of the nHAs can afford more space for cell growth, and HA particles with a smaller size show a stronger adhesion and can better penetrate into cells. The uptake of nHAs by cells is mainly through endocytosis, vesicle transport, or cell membrane indentation.[168] During this process, nHAs are partially dissolved by lysosomes to form solutes that contain Ca^{2+} and infiltrate into the cytoplasm; here the appropriate concentration of calcium ions is beneficial for the proliferation and differentiation of osteoblasts.[169] Additionally, the lower degree of crystallinity of nHA, compared to mHA, was one of the reasons why it could better promote osteoblastic proliferation.[170] However, other studies found that NP20 show the strongest inhibition effect on U2OS human osteosarcoma cells. This demonstrates that nHAs exhibit different biological activities on different cell lines. Additionally, the shape of nHAs affects their bioactivity: spherical particles show a better osteogenic effect than rod-shaped particles, presumably because well-organized spherical structures are beneficial for filopodia protrusion.[171] The cytotoxicity of nHAs was also evaluated. It was found that NP20 showed the lowest cytotoxicity, presumably because the dissolution of nHAs was inhibited owing to their small size. Here, the amounts of calcium and phosphate ions released into the cytoplasm are limited and the cell apoptosis caused by high ion concentrations is prevented.[172]

In addition to the exploration of the biological activity of nHAs, many studies have applied nHA for the treatment of bone-related diseases. Khajuria *et al.* prepared nitrogen-doped carbon dots that are bound with HA nanoparticles (NCDS-HA) using a hydrothermal co-precipitation technique. NCDS can bind HA through electrostatic interactions and hydrogen bonds. NCDS-HA can be used not only for cell imaging, but also to enhance the activity of alkaline phosphatase, mineralization, and expression of osteogenic genes in osteoblasts. Here, these nanoparticles are used for the diagnosis and treatment.[173] Soares *et al.* successfully prepared mesoporous HA nanoparticles with a diameter of 285 nm, a surface area of 103 $m^2\ g^{-1}$, and a mesoporous size of $\sim$2–8 nm. These mesoporous HA nanoparticles can be used for the treatment of bone cancer when coated with the anticancer drug vincristine (Table 2).[174]

3.2.2 Silica nanoparticles. Silica can improve the development and growth of bones. Therefore, silica nanoparticles with biological activities have great potential in bone tissue engineering.[175,176] Mesoporous silica nanoparticles (MSNPs) have attracted attention because of their adjustable pore structure and large surface area.[177–181] MSNPs have a high DLE, facile surface functionalization, good thermal and chemical stability, and low toxicity, making them valuable for biomedical applications.[182–186]

MSNPs are mostly synthesized with the sol–gel method;[187–189] here, the acid or base catalyzed hydrolysis and condensation of silicon alkoxide precursors around surfactants that act as structural templates to form oxide networks (colloidal solutions) is used. These precursors are dropwise added into the solution in order to obtain a dilute colloidal solution. When the sol–gel process occurs, these droplets will gradually transform into monodisperse silica nanospheres. The final mesoporous silica nanospheres are obtained by solvent extraction and surfactant removal. Conditions such as temperature, concentration, and the type of surfactant have a significant influence on the final morphology of the generated MSNPs.[181] The particle size, surface area, volume area, and the surface functionality of MSNPs, as well as the pore diameter, volume, and structure are highly adjustable. MSNPs with diameters of 50–300 nm are suitable for biological applications.[190] The presence of pores allows these MSNPs to

carry and release a large number of host molecules. However, the pore size limits the size of the molecules that can be used. Generally, the pore size can be adjusted around ~2–50 nm, depending on the synthesis conditions and the surfactant. MSNPs with small pore sizes are used as carriers of therapeutic drugs, while MSNPs with large pore sizes are used as carriers of proteins, enzymes, antibodies, nucleic acids, *etc.*[191] Additionally, the pore volume is one of the most important factors affecting the loading capacity of MSNPs. Most pore volumes of MSNPs are about 1 $cm^3\ g^{-1}$; however, some can reach 4.5 $cm^3\ g^{-1}$.[192] In addition to the diameter and volume, the structure of the pores can also impact the encapsulation and release of guest molecules. Presently, the type of pores includes a concentric circular shape, a cubic shape, a radial shape, a worm-like shape, *etc.* The silanol groups on the surface of MSNPs can react to form various functional groups, thus giving MSNPs various surface chemical properties, making them suitable for different functions.[193]

Ge *et al.* synthesized MSNPs coated with gold nanorods (Au@MSNs) *via* the sol–gel method, and incorporated the bone-targeting group zoledronic acid (ZOL) to the surface of MSNPs through an aminolysis reaction, to prepare bone-targeting MSNPs (Au@MSNs-ZOL).[194] The area of the mesoporous Au@MSNs surface structure reached 176 $cm^2\ g^{-1}$. This high surface area improved its binding ability towards ZOL, and the maximum incorporated ZOL amount was 167 $mg\ g^{-1}$. These Au@MSNs-ZOL can be used for photoacoustic imaging (PA) and photothermal therapy (PTT) in the presence of gold nanorods (Fig. 5). Irradiation of Au@MSNs-ZOL with near-infrared light led to an absorption peak at 808 nm and an increase in local temperature to 42.3 °C. *In vitro* experiments showed that ZOL could be released faster when the temperature increased during photothermal therapy. This responsive release did not only increase the cumulative amount of ZOL released at the irradiated sites, but also avoid the toxic side effects that are caused by the premature ZOL release. *In vivo* studies have shown that Au@MSNs-ZOL can rapidly target bone tissue and realize combined diagnosis and therapy of bone metastasis. Additionally, Au@MSNs-ZOL can be cleared by the liver and kidney over time.

Pasqua *et al.* applied surface functionalized MSNPs to encapsulate and deliver ibuprofen to the bone.[162] First, they

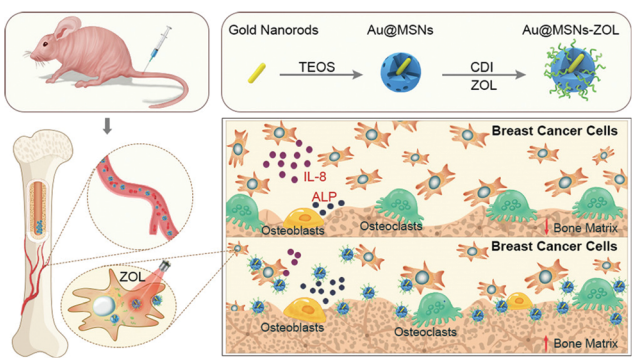

Fig. 5 Schematic diagram of the preparation and theranostic process of Au@MSNs-ZOL. Reproduced with permission from ref. 194. Copyright 2019 American Chemical Society.

modified cyanide groups on the outer surface of MSNPs to obtain MSNPS-CN, and these groups were hydrolyzed to obtain carboxylic groups (MSNPS-COOH). The bone-targeting ligand alendronate can be bound to the outer surface through electrostatic interactions to form the final bone-targeting MSNPs (MSN-COO-AL). The particle size of MSN-COO-AL ranges from 100 to 200 nm, and the mesoporous diameter is about 7 nm. They declared that the wide particle size distribution was caused by insufficient surfactant removal. 70% of the loaded ibuprofen could be released in 30 min and totally released after 120 min. They speculated that this rapid drug release was related to the small molecular size of ibuprofen (0.6 nm) and the relatively large mesoporous pore size. Additionally, they confirmed the bone-targeting properties of MSN-COO-AL by *in vitro* HA binding and demonstrated that these nanoparticles had no negative effect on normal human cell proliferation (Table 2).

3.2.3 Metal oxide nanoparticles. Iron oxide nanoparticles (IONPs) are suitable for biomedical applications, since iron is a necessary element in the body.[195–198] However, IONPs have active surfaces and the tendency to aggregate, leading to potential biotoxicity. Thus, preventing IONPs from aggregating and being oxidized by surface coating and chemical modifications is therefore crucial to increase their biocompatibility.[198,199] Additionally, surface coating and chemical modification can provide IONPs with multiple functions. Generally speaking, IONPs are core–shell nanoparticles consisting of an iron oxide core that is coated with organic (polyethylene glycol, chitosan, block polymers, *etc.*[200,201]) or inorganic (silicon, gold, calcium phosphate, *etc.*[202–204]) layers. The shell can consist of a single layer or multiple layers; each layer can be chemically modified to achieve multiple functions. The natural magnetic properties of IONPs have broad application prospects. An external magnetic field can generate magnetic induction among IONPs and form an internal nanoscale magnetic field. These magnetic fields can induce energy changes that can be used for the diagnosis and treatment of various diseases, for example, in magnetic resonance imaging (MRI)[205] and in magnetic hyperthermia.[206]

Doschak *et al.* reported a bone-targeting MRI contrast agent based on alendronic acid-modified superparamagnetic iron oxide nanoparticles (SPION-ALNs).[207] First, hydrophilic SPIONs with a controllable size were synthesized by the water-in-oil reverse micro-emulsion method, then the nanoparticle surface was coated with citric acid. This citric acid shell did not only provide binding sites for alendronic acid, but also enhanced the stability of SPION-ALNs (Fig. 6). The average diameter of these SPION-ALNs is 17 nm and the surface potential is −32 mV. These SPION-ALNs showed high bone affinity: the HA binding rate reached 65%; 95% of the SPION-ALNs remained attached to HA after 24 h. These SPION-ALNs can be used for the diagnosis of bone metabolic diseases and for observing the bone transitions.

Lou *et al.* constructed alendronate-conjugated, glucan-coated Fe_3O_4 nanoparticles (BIS/DEX/Fe_3O_4). The thermolysis of these nanoparticles at radiofrequency can be used to reduce the activity of osteoclasts.[208] First, Fe_3O_4 nanoparticles were

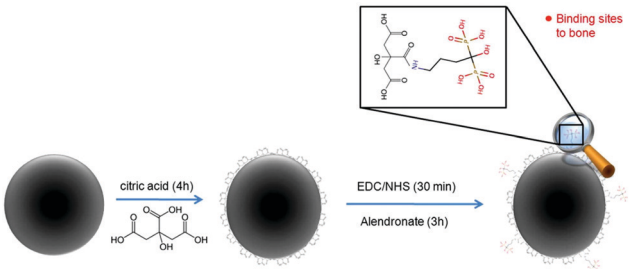

Fig. 6 Preparation of SPION-ALN and its bone-targeting site. Reproduced with permission from ref. 207. Copyright 2020 American Chemical Society.

synthesized using a chemical co-precipitation method. Afterwards, a dextran coating was applied on its surface, and these dextran-coated Fe_3O_4 nanoparticles (Dex/Fe_3O_4) greatly improved the biocompatibility. After that, these nanoparticles were modified with alendronate to form BIS/DEX/Fe_3O_4 with a bone-targeting ability. *In vivo* experiments showed that BIS/DEX/Fe_3O_4 successfully accumulated into the bone tissue. The local temperature increased by 7 °C after exposing BIS/DEX/Fe_3O_4 (20 mg mL^{-1}) to radiofrequency for 20 min, and the activity of osteoclasts was significantly inhibited. However, while this method did reduce the survival rate of osteoclasts, it did not affect the survival rate of osteoblasts. It was hypothesized that alendronate can promote the osteoclast uptake of BIS/DEX/Fe_3O_4. Therefore, the thermolysis of BIS/DEX/Fe_3O_4 acted mainly on osteoclasts and reduced their activity without breaking the balance of the bone metabolism.

It has been reported that titanium dioxide nanoparticles (TiO_2 NPs) can accelerate bone growth, and therefore they are widely used in bone tissue engineering.[209,210] ŁAncucka *et al.* doped TiO_2 NPs into collagen/chitosan hydrogels to prepare injectable skeletons that can be used for bone regeneration.[211] These injectable skeletons successfully induced bone mineralization and promoted the formation of apatite-like structures within bone tissues. The doped TiO_2 NPs have a significant effect on the swelling properties of the collagen/chitosan hydrogels. Additionally, the doped TiO_2 NPs also enhanced the hydrophilicity of the hydrogel and did not affect its biocompatibility. Ikono *et al.* doped TiO_2 NPs into chitosan scaffolds to form a chitosan–TiO_2 sponge (CTS). This CTS showed enhanced bone regeneration ability.[212] It was observed that TiO_2 NPs with intact pore structures and good connectivity distributed uniformly on the surface of the chitosan scaffolds. Obvious bone mineralization occurred on the surface of CTS when 50% of TiO_2 nanoparticles were added, indicating that CTS can significantly promote bone regeneration. Moreover, the addition of TiO_2 nanoparticles can also significantly increase the structural stability of chitosan scaffolds. It was found that the structure of CTS remained intact in simulated body fluids (SBFs) after two weeks; in contrast, common chitosan scaffolds collapsed within 7 days. It is noteworthy that TiO_2 NPs were also able to enhance the biocompatibility of the chitosan scaffold (Table 2).

Some other kinds of metal oxide nanoparticles and metal nanoparticles have also been used to diagnose and treat bone-related diseases.[29,213–216] Such nanoparticles have better mechanical properties than polymer nanoparticles.[217]

4. Biomedical applications of bone-targeting nanoparticles

4.1 Primary malignant bone tumors and bone metastasis

Malignant bone tumor is a general term for malignant tumors that grow in bone tissues. These tumors can be divided into primary malignant tumors and metastatic malignant tumors.[6,218] Primary malignant tumors include osteosarcoma, chondrosarcoma, fibrosarcoma, *etc.*, among which osteosarcoma ranks the third most common cancer with an unsatisfactory prognosis in adolescents.[219,220] Metastatic malignant tumors include lung cancer bone metastasis, kidney cancer bone metastasis, breast cancer bone metastasis, prostate cancer bone metastasis, *etc.* Bone metastatic tumors are more common than primary malignant tumors because they are one of the most common complications of a later-stage cancer.[11] Studies have shown that 65–80% of patients with later-stage breast and prostate cancers have bone metastasis and 35–42% of patients with later-stage thyroid, lung and renal cancers have bone metastasis.[221,222] After being invaded by malignant tumors, the physiological balance of bone tissue will be broken. These tumor cells can lead to an abnormal bone cell metabolism (in osteoblasts and osteoclasts), thus causing pathological bone damage, which, in turn, will promote the proliferation of tumor cells.[10,223] This 'vicious cycle' can eventually lead to bone-related complications such as bone pain, osteoarthritis, and fracture. Currently, the clinical treatment for malignant bone tumors includes surgical resection, chemotherapy, radiotherapy, *etc.*[224] Surgical resection is only suitable for the treatment of tumors at an early stage but not for multiple and aggressive malignant bone tumors. Systemic radiotherapy and chemotherapy can be used to treat multiple kinds of tumors; however, the therapeutic effect is often unsatisfactory. The main limitations are as follows: (1) radiotherapy and chemotherapy lack the bone targeting ability, and therefore it is difficult for therapeutics to accumulate at the tumor site. This results in low drug utilization and potential side effects on other tissues. (2) The bone marrow micro-environment can promote the proliferation and differentiation of tumor cells. The hard and dense cellular mineralized extracellular matrix inhibits the penetration of drugs into the tumor tissue. (3) Most bone metastases are drug-resistant tumors.[225] Bone-targeting nanoparticles can help small molecule drugs to accumulate at the bone tumor site, increase the stability of drugs during circulation and eliminate their side effects on other normal tissues.[9] Additionally, bone-targeting nanoparticles can also combine multiple treatment approaches to further improve the therapeutic effect for malignant bone tumors and tumor-related bone diseases.[226]

Duvall *et al.* prepared a kind of bone-targeting nanoparticles (BTNPs) for the loading and the targeted-delivery of small molecule Gli2 inhibitors (GANT58) for the inhibition of breast

cancer bone metastases and tumor-related bone damage (Fig. 7).[227] BTNPs were fabricated with the amphiphilic diblock copolymer poly-[(propylene sulfide)-*b*-(alendronate acrylamide-*co*-*N*,*N*-dimethylacrylamide)] [PPS-*b*-P(Aln-*co*-DMA)]. Here, a bulk solvent evaporation or nanoprecipitation method was used. GANT58-loaded BTNPs (GANT58-BTNPs) were prepared during this self-assembly process. They demonstrated that GANT58 can inhibit the transcription factor Gli2 and consequently the PTHrP expression by tumor cells, reducing tumor-related bone resorption and disrupting the 'vicious cycle' between the bone tissue and tumor.[228,229] They synthesized a series of PPS-*b*-P(Aln-*co*-DMA) with different alendronate contents to optimize the ability of BTNPs to target tumor-associated bones. This is based on the combination of active bone binding and nonspecific tumor accumulation (enhanced permeation and retention effect). They found that a complete alendronate modification provides BTNPs with strong bone affinity. However, this modification makes BTNPs extremely negatively charged, resulting in a short circulation time, increased liver uptake, and less distribution in bone metastatic tumors.[230] The optimum balance of systemic pharmacokinetics and bone targeting and the highest bony/hepatic biological distribution ratio were achieved when the alendronate content was 10%. The treatment effect with this alendronate content was examined, and it was found that the area of bone damage was reduced 0.3-fold, and that the bone volume fraction of tibia increased 2.5-fold. GANT58-BTNPs specifically inhibited the proliferation of bone tumors and prevented tumor-related bone damage. The authors assumed that the combination of GANT58-BTNPs with chemotherapy drugs would achieve better therapeutic effects.

Wang *et al.* prepared bone-targeting Ag_2S nanoparticles (ALD/DOX@Ag_2S) by modifying the surface of Ag_2S with the bone-targeting ligand alendronate (ALD). During preparation the anticancer drug DOX was encapsulated for treating bone metastasis and tumor-induced osteolysis.[215] Afterwards, DSPE-PEG-COOH was used to coat these nanoparticles to obtain a higher hydrophilicity and to provide binding sites for alendronate. The hydrodynamic diameter of these ALD/DOX@Ag_2S was about 110 nm, and approximately 38 alendronate units were grafted on the surface of each particle. DOX was loaded within the hydrophobic layer with a DLE of about 85%. ALD/DOX@Ag_2S maintained high colloidal stability in PBS buffer, fetal bovine serum, and DMEM culture medium for more than 96 h at 37 °C. *In vitro* experiments showed that the HA binding ability of these nanoparticles is positively correlated with concentration. Additionally, good bone affinity was maintained in complex physiological environments with a variety of biological molecules. ALD/DOX@Ag_2S also showed tumor-responsive drug release. The cumulative DOX release was only 15% within 96 hours in a normal physiological environment (pH = 7.4); however, the cumulative DOX release reached 85% within 48 hours in a tumor-mimicking environment. *In vivo* studies showed that ALD/DOX@Ag_2S preferentially distributed in the spine, leg bone, and tail of mice 12 hours after intravenous injection. It was found that ALD/DOX@Ag_2S effectively

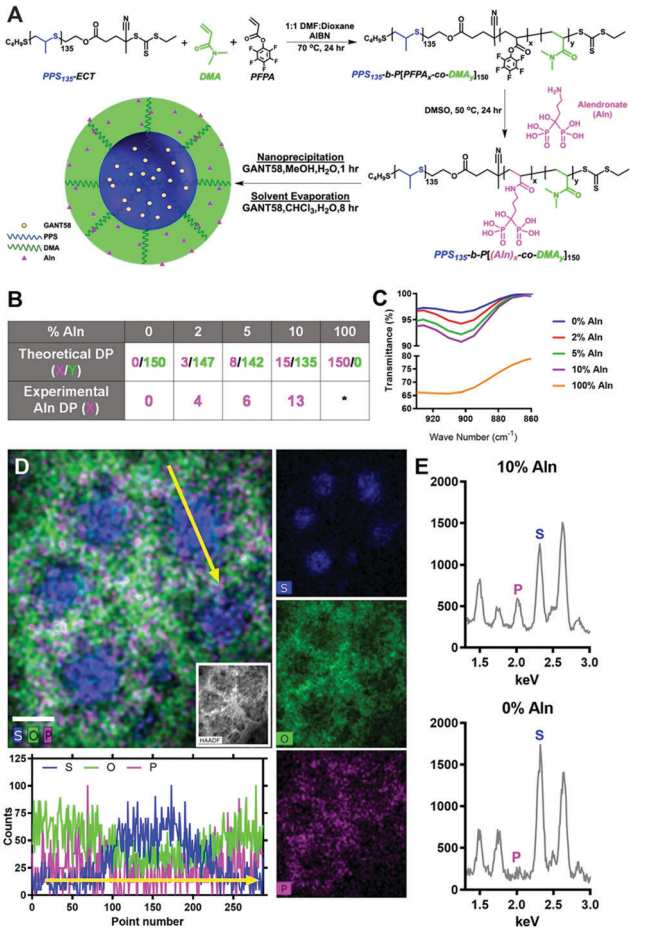

Fig. 7 Synthesis and structural characterization of GANT58-BTNPs. Reproduced with permission from ref. 227. Copyright 2020 American Chemical Society.

suppressed tumor growth and extended the survival period of mice to 120 days after tumor transplantation. Additionally, ALD/DOX@Ag_2S can significantly inhibit the activity of osteoclasts, enhance bone mineralization, and significantly increase the volume of trabecular bone.

Bu *et al.* designed zoledronic acid (ZA)-modified, plumbagin (PL)-loaded bimodal mesoporous silica covered gadolinium(III) upconversion nanoparticles (PL-Gd-UCNP@ZA-PAA, PUCZPs) for the diagnosis and treatment of breast cancer bone metastases (Fig. 8).[231] These multifunctional nanoparticles can target osteocytes and release plumbagin in a pH-responsive way to inhibit cancer growth and invasion of healthy tissues. Osteocytes play a regulatory role in early stage bone metastasis by promoting the generation of osteoclasts through the expression of the growth factor RANKL and mediating tumor-related bone damage. In early studies, they found that UCNPs could be used for radio-/photodynamic endonuclear treatment that is guided by bimodal magnetic/luminescence imaging instruction.[232] On this basis, they introduced the bone-targeting ligand zoledronic acid (ZA) to UCNPs for the diagnosis and treatment of bone metastases. Experimental results showed that PUCZPs exhibit upconversion luminescence (UCL) performance under

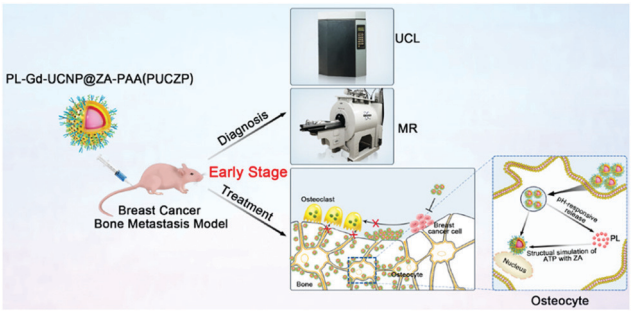

Fig. 8 Schematic diagram of PUCZP for the diagnosis and treatment of breast cancer with bone metastases. Reproduced with permission from ref. 231. Copyright 2019 American Chemical Society.

980 nm laser irradiation. An increased PUCZP concentration led to brighter T_1-weighted signals. Additionally, ZA and the anticancer drug plumbagin synergistically inhibited the expression of RANKL and sclerostin in bone cells, thus effectively inhibiting osteoclast development mediated by bone cells, breaking the 'vicious cycle' between bone metastases and bone cells and inhibiting tumor growth.

4.2 Osteoporosis

With the aging of the population and the general increase of people's lifetime, osteoporosis has become a medical and socioeconomic threat.[4,233,234] Osteoporosis is a systemic decrease in bone density, strength, and toughness, resulting in a damaged bone microstructure and risk of fracture. The evaluation of osteoporosis is based on bone mineral density analysis. The World Health Organization defines bone mineral density with a *T*-score, where a score less than 2.5 indicates osteoporosis.[235,236] However, it should be noted that it is usually unnoticed until the first fracture has happened, since the decrease in bone mineral density (BMD) is asymptomatic.[237] The incidence of fractures in patients with osteoporosis is as high as 40% and fractures frequently occur in the spine, hip, or wrist. The patients' mortality rate increases by up to 20% one year after the fracture occurred, as chronic immobilization may lead to complications such as pneumonia or thromboembolic disease.[238] Dual X-ray absorptiometry (DXA) measurement of bone mineral density can effectively diagnose osteoporosis and predict the risk of fracture.[239] However, this method has some limitations: DXA can measure regional bone mineral density, but cannot distinguish subtle bone structures (such as the cortical bone and the trabecular bone).[240] At present, drugs for the treatment of osteoporosis can be divided into two main categories: drugs that prevent bone resorption and drugs that promote bone formation. Anti-resorption drugs mainly include bisphosphonates, raloxifene, strontium ranelate, denosumab, *etc.*, while bone formation drugs mainly include osteogenic protein (BMP-2), simvastatin, parathyroid hormone (PTH 1–84) and this hormone's N-terminal fragment teriparatide (PTH 1–34), *etc.*[241,242] However, most of them can cause undesired side effects, thus affecting the potential long-term use and therapeutic effect.[243,244] In recent years, many nanotechnologies and nanomaterials have been applied for the treatment of osteoporosis and the research on bone-targeting nanoparticles has also attracted a tremendous amount of attention.[245,246] The application of bone-targeting nanoparticles in the diagnosis and treatment of osteoporosis can significantly enhance these treatment methods.

Wang *et al.* combined the bone-targeting peptide Asp_6 with stearic acid-polyethylene glycol 2000 (SA-PEG2000-NH_2) to prepare bone-targeting lipid nanoparticles (SIM/ASP_6-LNPs), which are capable of the targeted-delivery of SIM for the treatment of osteoporosis (Fig. 9).[247] The diameter of these ASP_6-LNPs is 100 nm, and the particle size slightly increased after SIM loading. The DLE of SIM was as high as 97.3% and the cumulative drug release could reach 70% within 48 hours. ASP_6-LNPs were preferentially consumed by MC3T3-E1 osteoblasts and low cytotoxicity was observed. Additionally, SIM/ASP_6-LNPs successfully induced the differentiation and mineralization of these MC3T3-E1 osteoblasts and promoted bone mineralization. Compared with free SIM and SIM/LNPs without bone-targeting ligands, SIM/ASP_6-LNPs could effectively increase the bone density to a normal value. The good biocompatibility of ASP_6-LNPs increased the circulation and the stability of SIM. The bone-targeting ability allowed efficient osteoporosis treatment while reducing the negative side effects of SIM on healthy tissues.

Devarajan *et al.* prepared an HA nanoparticle loaded with salmon calcitonin (SCT) for the treatment of osteoporosis that can be orally administered (Fig. 10).[248] First, they prepared HA nanoparticles (HAP NPs) using an aqueous precipitation method. These particles were coated with the ionic surfactant sodium oleate. Excess surfactant arranged as a multilayer structure around the HA NPs to improve the surface stability of the particles, preventing aggregation and precipitation. Additionally, the negatively-charged sodium oleate layers can promote the deposition of positively-charged SCT on the surface of HAP-NPs. The particle size of these SCT-HAP-NPs was about 100 nm and allowed, therefore, passage through the bone capillary wall with pores of about ~80–100 nm, to reach the targeted site. Additionally, this size ensured a long *in vivo*

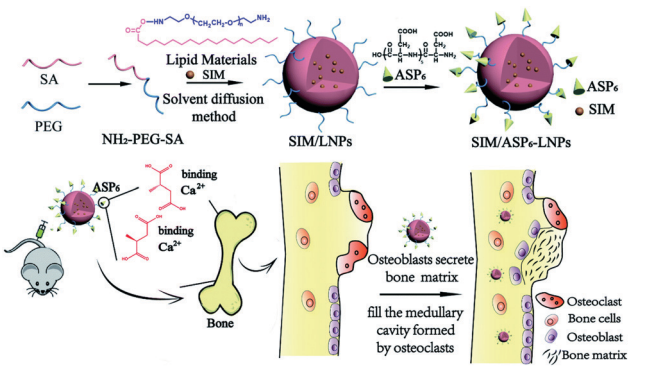

Fig. 9 Preparation of SIM/Asp_6-LNPs and mechanism of osteoporosis treatment. Reproduced with permission from ref. 247. Copyright 2020 The Royal Society of Chemistry.

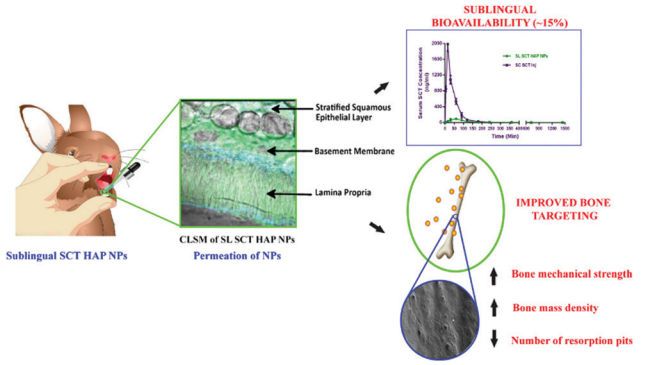

Fig. 10 SCT-HAP-NPs showed good sublingual permeability and bone targeting ability. Reproduced with permission from ref. 248. Copyright 2020 Elsevier Ltd.

circulation time. These particles could efficiently load SCT with a DLE of 85%. Of loaded calcitonin, 85% could be gradually released in 24 h. Confocal laser scanning microscopy showed that SCT-HAP-NPs could effectively penetrate the deep layer of mucosa, while free SCT only remained at the surface area. It was assumed that the suitable size, good surface stability, and carboxyl groups in the sodium oleate layer simultaneously promoted the permeability of SCT-HAP-NPs to mucosa. *In vivo* studies demonstrated that orally administered SCT-HAP-NPs achieved a relative bioavailability of ~15% compared to intravenous administration. This significantly increased the mass and strength of the bone, reducing bone erosion and adjusting osteoporosis related serum biomarkers.

Hasirci *et al.* used PLGA nanoparticles for the delivery of siRNA. Here, PLGA nanoparticles were modified with the bone targeting group elastin-like recombinamer (ELR) for the treatment of osteoporosis.[249] The cationic polymer polyethylenimine (PEI) was used to form a complex with siRNA (PEI:siRNA) through electrostatic interactions. This complex protects siRNA from the extracellular nuclease and neutralizes the negatively charged siRNA, allowing an enhanced siRNA cell uptake. Additionally, PEI can also trigger a proton sponge effect, helping siRNA to escape from endosomes. Unfortunately, PEI is cytotoxic, and therefore utilizing ELR-PLGA nanoparticles with good biocompatibility is essential to reduce the cytotoxicity and enhance bone adsorption. These ELR-PLGA nanoparticles were about 220 nm in diameter, and the DLE of PEI:siRNA was about 48%. The cumulative release of PEI:siRNA could reach 80% in 15 days. Cell experiments showed that encapsulated PEI:siRNA PLGA nanoparticles were non-cytotoxic and could be internalized by the osteoclast precursor cells RAW264.7. This approach significantly reduced RANK mRNA levels and hindered its differentiation and activity.[250]

4.3 Diagnosis and detection of bone diseases

Timely and accurate diagnosis is critical for the treatment of bone-related diseases. The diagnosis of osteoporosis mainly depends on the measurement of BMD (T-score < 2.5 indicates osteoporosis). A 10-year probability of fracture can be determined to establish intervention thresholds.[251] DXA is considered as the gold standard for measuring bone mineral density.[236] Compared to DXA, which requires indirect calculation to obtain the BMD value, quantitative computed tomography (CT) can directly measure the value of BMD. CT is also insensitive to the interference of some degenerative diseases.[251] Presently, CT has been applied for the detection of bone mineral density in the appendicular skeleton and spine. Besides, CT can also be used to monitor the treatment outcomes since cancellous bones are more sensitive than the cortical bone for this measurement. However, some drawbacks from CT should be considered: ionic radiation exposure, poor quality control, and high cost. Radiography is another way of diagnosing osteoporosis. Here, special symptoms associated with osteoporosis can be directly observed by using X-rays, and this can help to predict the stage of the disease and detect potential fracture sites in advance.[251] Quantitative ultrasound can be used to access the skeleton status in osteoporosis: broad-band ultrasound attenuation and ultrasound velocity are the commonly used methods. However, ultrasonic measurements cannot be used to diagnose osteoporosis.

In the diagnosis of bone tumors, the clinically used methods include CT, bone radiography, MRI, and fusion imaging methods, such as SPECT/CT, PET/CT and PET/MRI.[252–257] CT can offer high resolution imaging of the cortical bone and the trabecular structure. This method is more sensitive for the detection of malignant bone tumors involving cortical bones, and osteolytic and osteoplastic metastases in soft tissues. CT can also be used to evaluate the stability of bone structures around tumor lesions, assisting bone radiography or MRI in analyzing abnormal bone structures.[258] Bone radiography is suitable for the detection of malignant bone tumors with abnormal metabolism, such as bone metastasis of prostate cancer and breast cancer, osteosarcoma, *etc.*[259] MRI with high spatial resolution and high bone/soft tissue contrast has inherent advantages for bone imaging. Moreover, MRI can be used to obtain information of bone metabolism and highlight the interaction of drugs with bone tissue, thus achieving the dynamic monitoring of the treatment process. Additionally, MRI is radiation free so it causes less damage to the body compared to CT and radiography.[260] Hybrid imaging techniques can also be used and achieve better diagnostic effects. This approach can be used to image the bone tissue and locate the tumor simultaneously.[261] Widely used examples of such hybrid techniques include SPECT/CT, PET/CT, and PET/MRI.[252]

Nanotechnology has shown great potential in improving the diagnostic sensitivity.[8] The application of bone-targeting nanoparticles in bone disease diagnosis has achieved significant results. The use of nanoparticles for integrated diagnosis and treatment has drawn extensive attention.[129,262,263] Roeder *et al.* designed gold nanoparticles (Au NPs) as a potential bone damage-specific X-ray contrast agent. This approach is non-destructive, non-invasive, and provides three-dimensional (3-D) detection and imaging of micro-damage within the bone tissue.[264] Here, gold nanoparticles with a diameter of ~15–40 nm were prepared with a citrate reduction reaction. Subsequently they were functionalized with the bone-targeting

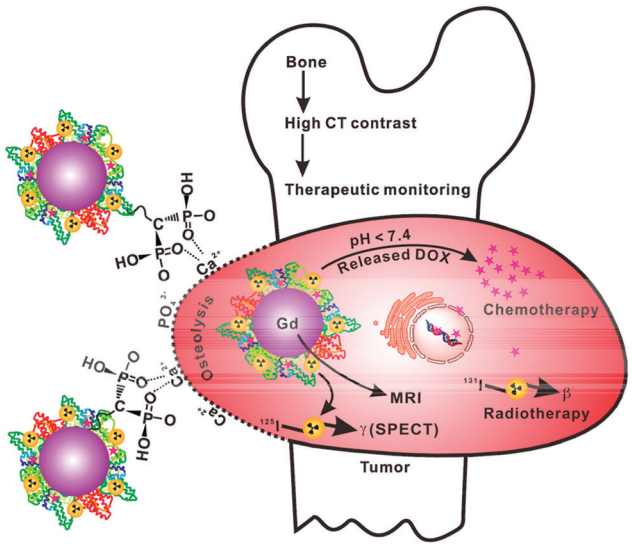

Fig. 11 Schematic diagram of ALN-GDOX NPs for *in vivo* MRI and SPECT/CT. Reproduced with permission from ref. 265. Copyright 2020 American Chemical Society.

peptide glutamic acid to target damaged bone tissue. Compared with clinical bone contrast agents, the bone-targeting gold nanoparticles have better biocompatibility and greater X-ray attenuation. Sheng *et al.* reported alendronate-functionalized albumin-based gadolinium oxide nanoparticles (ALN-GDOX NPs) for enhanced MRI imaging and SPECT/CT imaging of bone tumors (Fig. 11).[265] They demonstrated that ALN-GDOX NPs can realize the combination of *in vivo* targeted imaging and radio-chemotherapy for bone tumors as a theranostic platform.

Qu *et al.* reported a rare earth doped DSPE-mPEG-coated nano-particle (RENPs@DSPE-mPEG) with bone affinity that can be used as a near-infrared II (NIR-II) fluorescence imaging agent for bone imaging and the diagnosis of bone-related diseases.[30] NIR-II fluorescence imaging exhibits higher signal-to-noise ratio and tissue penetration capability compared to visible light imaging and NIR-I fluorescence imaging. Rare earth doped nanoparticles (RENPs) are composed of lanthanide ions that are loaded within an inorganic crystalline host matrix which can emit near-infrared light. These nanoparticles have a large Stokes shift, a narrow emission peak, a long service life, and good photo-stability. However, the poor water-solubility of RENPs hinders their further functionalization in biological applications. DSPE-mPEG was used to coat RENPs to increase their surface hydrophilicity.

They found that RENPs@DSPE-mPEG have a natural bone affinity: no bone-targeting ligand was required. It was assumed that this is mainly because of the similar structure of RENPs to that of HA crystals. When excited with an 808 nm laser, RENPs@DSPE-mPEG exhibited bimodal fluorescence emission at both 1064 and 1345 nm. Within the NIR-II window, imaging at a longer wavelength (1345 nm) provides higher resolution and signal-to-noise ratio. The total body clearance of RENPs@DSPE-mPEG can be achieved after a week, which provides possibilities for clinical applications.

5. Perspective and conclusion

Bone-targeting nanoparticles and their applications in bone-related diseases have attracted more and more attention. The specific bone affinity of bone-targeting nanoparticles comes from bone-targeting ligands. The targeting sites of these bone targeting ligands vary from bone surface targeting to bone cell targeting, and they functioned in different ways. Many types of nanoparticles, organic and inorganic ones, have been applied for the design of bone-targeting nanoparticles. Some of them have inherent bone targeting ability, and thus no bone targeting ligands are needed. Bone-targeting nanoparticles have been widely used in bone tissue engineering, the diagnosis and treatment of bone metastasis and osteoporosis, *etc.* Promising outcomes have been achieved as bone-targeting nanoparticles do not only increase the circulation time and bone tissue accumulation of agents, but also reduce the side effects caused by systemic administration. Additionally, bone-targeting nanoparticles can incorporate multiple treatments such as PTT and PDT.[266] They have also been used as contrast agents for MRI, SPECT, CT, and hybrid imaging techniques for the diagnosis of bone-related diseases. Hence, bone-targeting nanoparticles provide potential possibilities for clinical applications.

However, there is still a long way to go to narrow the large gap between scientific research and clinical use. Evaluation of the biosafety of these bone-targeting nanoparticles in order to achieve biocompatibility and the desired activity is of vital importance. Bone-targeting ligands such as bisphosphonates and tetracyclines are clinical medication and have been used for decades. Organic nanoparticles such as lipids, polymers and protein-based nanoparticles are the major categories that are clinically approved. Inorganic nanoparticles, such as gold and iron oxide nanoparticles, have been found to exhibit toxicity both *in vitro* and *in vivo*. But these harmful effects can be reduced by surface modification. On this basis, bisphosphonate/tetracycline modified lipids, polymers, and protein-based bone-targeting nanoparticles are most likely to be used first in clinical trials and then in the human body. With the introduction of safer nanomaterials and optimal design, we will witness an increasing number of bone-targeting nanoparticles entering the clinic in the future.

Conflicts of interest

There are no conflicts to declare.

Acknowledgements

This work was supported by the National Natural Science Foundation of China (21925505), Shanghai International Scientific Collaboration Fund (21520710100), and China Postdoctoral Science Foundation (2020M671197). J. D. is a recipient of National Science Fund for Distinguished Young Scholars.

Notes and references

1 S. C. Marks, Jr. and S. N. Popoff, Bone cell biology: the regulation of development, structure, and function in the skeleton, *Am. J. Anat.*, 1988, **183**, 1–44.

2 F. Betts, N. C. Blumenthal and A. S. Posner, Bone mineralization, *J. Cryst. Growth*, 1981, **53**, 63–73.

3 T. Sozen, L. Ozisik and N. C. Basaran, An overview and management of osteoporosis, *Eur. J. Rheumatol. Inflammation*, 2017, **4**, 46–56.

4 T. D. Rachner, S. Khosla and L. C. Hofbauer, Osteoporosis: now and the future, *Lancet*, 2011, **377**, 1276–1287.

5 G. Ottaviani and N. Jaffe, The epidemiology of osteosarcoma, *Cancer Treat. Res.*, 2009, **152**, 3–13.

6 F. Macedo, K. Ladeira, F. Pinho and N. Saraiva, N. Bonito, L. Pinto and F. Goncalves, Bone metastases: an overview, *Oncol. Rev.*, 2017, **11**, 43–49.

7 R. E. Coleman, Clinical features of metastatic bone disease and risk of skeletal morbidity, *Clin. Cancer Res.*, 2006, **12**, 6243s–6249s.

8 R. van der Meel, E. Sulheim, Y. Shi, F. Kiessling, W. J. M. Mulder and T. Lammers, Smart cancer nanomedicine, *Nat. Nanotechnol.*, 2019, **14**, 1007–1017.

9 A. Lipton, Future treatment of bone metastases, *Clin. Cancer Res.*, 2006, **12**, 6305s–6308s.

10 J. Fornetti, A. L. Welm and S. A. Stewart, Understanding the bone in cancer metastasis, *J. Bone Miner. Res.*, 2018, **33**, 2099–2113.

11 K. N. Weilbaecher, T. A. Guise and L. K. McCauley, Cancer to bone: a fatal attraction, *Nat. Rev. Cancer*, 2011, **11**, 411–425.

12 J. S. Ni, Y. X. Li, W. T. Yue, B. Liu and K. Li, Nanoparticle-based cell trackers for biomedical applications, *Theranostics*, 2020, **10**, 1923–1947.

13 C. D. Spicer, C. Jumeaux, B. Gupta and M. M. Stevens, Peptide and protein nanoparticle conjugates: versatile platforms for biomedical applications, *Chem. Soc. Rev.*, 2018, **47**, 3574–3620.

14 F. Y. Li, J. X. Lu, X. Q. Kong, T. Hyeon and D. S. Ling, Dynamic nanoparticle assemblies for biomedical applications, *Adv. Mater.*, 2017, **29**, 1605897.

15 H. Cheng, A. Chewla, Y. F. Yang, Y. X. Li, J. Zhang, H. L. Jang and A. Khademhosseini, Development of nanomaterials for bone-targeted drug delivery, *Drug Discovery Today*, 2017, **22**, 1336–1350.

16 S. G. Rotman, D. W. Grijpma, R. G. Richards, T. F. Moriarty, D. Eglin and O. Guillaume, Drug delivery systems functionalized with bone mineral seeking agents for bone targeted therapeutics, *J. Controlled Release*, 2018, **269**, 88–99.

17 C. Shi, T. T. Wu, Y. He, Y. Zhang and D. H. Fu, Recent advances in bone-targeted therapy, *Pharmacol. Ther.*, 2020, **207**, 107473.

18 W. M. Pierce, Jr. and L. C. Waite, Bone-targeted carbonic anhydrase inhibitors: effect of a proinhibitor on bone resorption in vitro, *Proc. Soc. Exp. Biol. Med.*, 1987, **186**, 96–102.

19 R. A. Nadar, N. Margiotta, M. Iafisco, J. J. J. P. van den Beucken, O. C. Boerman and S. C. G. Leeuwenburgh, Bisphosphonate-functionalized imaging agents, antitumor agents and nanocarriers for treatment of bone cancer, *Adv. Healthcare Mater.*, 2017, **6**, 1601119.

20 J. S. Barbosa, F. A. A. Paz and S. S. Braga, Bisphosphonates, old friends of bones and new trends in clinics, *J. Med. Chem.*, 2021, **64**, 1260–1282.

21 H. H. Van Acker, S. Anguille, Y. Willemen, E. L. Smits and V. F. Van, Tendeloo, Bisphosphonates for cancer treatment: mechanisms of action and lessons from clinical trials, *Pharmacol. Ther.*, 2016, **158**, 24–40.

22 T. Sekido, N. Sakura, Y. Higashi, K. Miya, Y. Nitta, M. Nomura, H. Sawanishi, K. Morito, Y. Masamune, S. Kasugai, K. Yokogawa and K. Miyamoto, Novel drug delivery system to bone using acidic oligopeptide: pharmacokinetic characteristics and pharmacological potential, *J. Drug Targeting*, 2001, **9**, 111–121.

23 W. X. Cheng, Y. Yue, W. B. Fan, Y. P. Hu, X. L. Wang, X. H. Pan, X. X. Zhou, L. Qin and P. Zhang, Effects of tetracyclines on bones: an ambiguous question needs to be clarified, *Pharmazie*, 2012, **67**, 457–459.

24 T. M. Willson, P. S. Charifson, A. D. Baxter and N. G. Geddie, Bone targeted drugs. 1. Identification of heterocycles with hydroxyapatite affinity, *Bioorg. Med. Chem. Lett.*, 1996, **6**, 1043–1046.

25 C. Liang, B. S. Guo, H. Wu, N. S. Shao, D. F. Li, J. Liu, L. Dang, C. Wang, H. Li, S. H. Li, W. K. Lau, Y. Cao, Z. J. Yang, C. Lu, X. J. He, D. W. T. Au, X. H. Pan, B. T. Zhang, C. W. Lu, H. Q. Zhang, K. M. Yue, A. R. Qian, P. Shang, J. K. Xu, L. B. Xiao, Z. X. Bian, W. H. Tan, Z. C. Liang, F. C. He, L. Q. Zhang, A. P. Lu and G. Zhang, Aptamer-functionalized lipid nanoparticles targeting osteoblasts as a novel RNA interference-based bone anabolic strategy, *Nat. Med.*, 2015, **21**, 288–294.

26 J. J. Shi, J. Sun, W. Zhang, H. Liang, Q. Shi, X. R. Li, Y. Y. Chen, Y. Zhuang and J. W. Dai, Demineralized bone matrix scaffolds modified by CBD-SDF-1 alpha promote bone regeneration via recruiting endogenous stem cells, *ACS Appl. Mater. Interfaces*, 2016, **8**, 27511–27522.

27 S. Shi, W. Jiang, T. Zhao, K. E. Aifantis, H. Wang, L. Lin, Y. Fan, Q. Feng, F. Z. Cui and X. Li, The application of nanomaterials in controlled drug delivery for bone regeneration, *J. Biomed. Mater. Res., Part B*, 2015, **103**, 3978–3992.

28 L. A. Chen, J. M. Mccrate, J. C. M. Lee and H. Li, The role of surface charge on the uptake and biocompatibility of hydroxyapatite nanoparticles with osteoblast cells, *Nanotechnology*, 2011, **22**, 105708.

29 Y. D. Kwon, D. H. Yang and D. W. Lee, A titanium surface-modified with nano-sized hydroxyapatite and simvastatin enhances bone formation and osseintegration, *J. Biomed. Nanotechnol.*, 2015, **11**, 1007–1015.

30 S. Q. He, S. Chen, D. F. Li, Y. F. Wu, X. Zhang, J. F. Liu, J. Song, L. W. Liu, J. L. Qu and Z. Cheng, High affinity to skeleton rare earth doped nanoparticles for near-infrared II imaging, *Nano Lett.*, 2019, **19**, 2985–2992.

31 H. Fleisch and S. Bisaz, Isolation from urine of pyrophosphate, a calcification inhibitor, *Am. J. Physiol.*, 1962, **203**, 671–675.
32 H. Fleisch, J. Maerki and R. G. Russell, Effect of pyrophosphate on dissolution of hydroxyapatite and its possible importance in calcium homeostasis, *Proc. Soc. Exp. Biol. Med.*, 1966, **122**, 317–320.
33 M. D. Francis, R. G. Russell and H. Fleisch, Diphosphonates inhibit formation of calcium phosphate crystals in vitro and pathological calcification in vivo, *Science*, 1969, **165**, 1264–1266.
34 D. Fernandez, D. Vega and A. Goeta, The calcium-binding properties of pamidronate, a bone-resorption inhibitor, *Acta Crystallogr., Sect. C: Cryst. Struct. Commun.*, 2002, **58**, m494–m497.
35 D. Fernandez, D. Vega and A. Goeta, Alendronate zwitterions bind to calcium cations arranged in columns, *Acta Crystallogr., Sect. C: Cryst. Struct. Commun.*, 2003, **59**, m543–m545.
36 M. V. Lee, E. M. Fong, F. R. Singer and R. S. Guenette, Bisphosphonate treatment inhibits the growth of prostate cancer cells, *Cancer Res.*, 2001, **61**, 2602–2608.
37 D. E. Hughes, K. R. Wright, H. L. Uy, A. Sasaki, T. Yoneda, G. D. Roodman, G. R. Mundy and B. F. Boyce, Bisphosphonates promote apoptosis in murine osteoclasts in-vitro and in-vivo, *J. Bone Miner. Res.*, 1995, **10**, 1478–1487.
38 D. K. Wysowski, Reports of esophageal cancer with oral bisphosphonate use, *N. Engl. J. Med.*, 2009, **360**, 89–90.
39 E. Vanbeek, M. Hoekstra, M. Vanderuit, C. Lowik and S. Papapoulos, Structural requirements for bisphosphonate aactions in-vitro, *J. Bone Miner. Res.*, 1994, **9**, 1875–1882.
40 S. E. Papapoulos, Bisphosphonate actions: physical chemistry revisited, *Bone*, 2006, **38**, 613–616.
41 F. H. Ebetino, A. M. L. Hogan, S. T. Sun, M. K. Tsoumpra, X. C. Duan, J. T. Triffitt, A. A. Kwaasi, J. E. Dunford, B. L. Barnett, U. Oppermann, M. W. Lundy, A. Boyde, B. A. Kashemirov, C. E. McKenna and R. G. G. Russell, The relationship between the chemistry and biological activity of the bisphosphonates, *Bone*, 2011, **49**, 20–33.
42 A. A. Reszka and G. A. Rodan, Nitrogen-containing bisphosphonate mechanism of action, *Mini-Rev. Med. Chem.*, 2004, **4**, 711–719.
43 E. Puljula, P. Turhanen, J. Vepsalainen, M. Monteil, M. Lecouvey and J. Weisell, Structural requirements for bisphosphonate binding on hydroxyapatite: NMR study of bisphosphonate partial esters, *ACS Med. Chem. Lett.*, 2015, **6**, 397–401.
44 R. G. G. Russell, M. J. Rogers, J. C. Frith, S. P. Luckman, F. P. Coxon, H. L. Benford, P. I. Croucher, C. Shipman and H. A. Fleisch, The pharmacology of bisphosphonates and new insights into their mechanisms of action, *J. Bone Miner. Res.*, 1999, **14**, 53–65.
45 G. H. Nancollas, R. Tang, R. J. Phipps, Z. Henneman, S. Gulde, W. Wu, A. Mangood, R. G. G. Russell and F. H. Ebetino, Novel insights into actions of bisphosphonates on bone: differences in interactions with hydroxyapatite, *Bone*, 2006, **38**, 617–627.
46 R. G. G. Russell, Bisphosphonates: the first 40 years, *Bone*, 2011, **49**, 2–19.
47 R. G. G. Russell, N. B. Watts, F. H. Ebetino and M. J. Rogers, Mechanisms of action of bisphosphonates: similarities and differences and their potential influence on clinical efficacy, *Osteoporosis Int.*, 2008, **19**, 733–759.
48 P. Canepa, F. Chiatti, M. Corno, Y. Sakhno, G. Martra and P. Ugliengo, Affinity of hydroxyapatite (001) and (010) surfaces to formic and alendronic acids: a quantum-mechanical and infrared study, *Phys. Chem. Chem. Phys.*, 2011, **13**, 1099–1111.
49 R. Bosco, M. Iafisco, A. Tampieri, J. A. Jansen, S. C. G. Leeuwenburgh and J. J. J. P. van den Beucken, Hydroxyapatite nanocrystals functionalized with alendronate as bioactive components for bone implant coatings to decrease osteoclastic activity, *Appl. Surf. Sci.*, 2015, **328**, 516–524.
50 H. Hirabayashi, T. Sawamoto, J. Fujisaki, Y. Tokunaga, S. Kimura and T. Hata, Relationship between physicochemical and osteotropic properties of bisphosphonic derivatives: rational design for osteotropic drug delivery system (ODDS), *Pharm. Res.*, 2001, **18**, 646–651.
51 C. Reyes, M. Hitz, D. Prieto-Alhambra and B. Abrahamsen, Risks and benefits of bisphosphonate therapies, *J. Cell. Biochem.*, 2016, **117**, 20–28.
52 G. A. Schmidt, K. E. Horner, D. L. McDanel, M. B. Ross and K. G. Moores, Risks and benefits of long-term bisphosphonate therapy, *Am. J. Health-Syst. Pharm.*, 2010, **67**, 994–1001.
53 S. P. Luckman, D. E. Hughes, F. P. Coxon, R. G. G. Russell and M. J. Rogers, Nitrogen-containing bisphosphonates inhibit the mevalonate pathway and prevent post-translational prenylation of GTP-binding proteins, including Ras, *J. Bone Miner. Res.*, 1998, **13**, 581–589.
54 S. Boissier, M. Ferreras, O. Peyruchaud, S. Magnetto, F. H. Ebetino, M. Colombel, P. Delmas, J. M. Delaisse and P. Clezardin, Bisphosphonates inhibit breast and prostate carcinoma cell invasion, an early event in the formation of bone metastases, *Cancer Res.*, 2000, **60**, 2949–2954.
55 D. J. Papachristou, E. K. Basdra and A. G. Papavassiliou, Bone metastases: molecular mechanisms and novel therapeutic interventions, *Med. Res. Rev.*, 2012, **32**, 611–636.
56 M. Fragni, S. A. Bonini, P. Bettinsoli, S. Bodei, D. Generali, A. Bottini, P. F. Spano, M. Memo and S. Sigala, The miR-21/PTEN/Akt signaling pathway is involved in the anti-tumoral effects of zoledronic acid in human breast cancer cell lines, *Naunyn-Schmiedeberg's Arch. Pharmacol.*, 2016, **389**, 529–538.
57 J. Schilcher, Bisphosphonate use and atypical fractures of the femoral shaft, *N. Engl. J. Med.*, 2012, **367**, 582.
58 M. A. Perazella and G. S. Markowitz, Bisphosphonate nephrotoxicity, *Kidney Int.*, 2008, **74**, 1385–1393.
59 S. L. Ruggiero, Bisphosphonate-related osteonecrosis of the jaw: an overview, *Ann. N. Y. Acad. Sci.*, 2011, **1218**, 38–46.

60 I. Chopra and M. Roberts, Tetracycline antibiotics: mode of action, applications, molecular biology, and epidemiology of bacterial resistance, *Microbiol. Mol. Biol. Rev.*, 2001, **65**, 232–260.
61 X. G. Liu, D. L. Huang, C. Lai, G. M. Zeng, L. Qin, C. Zhang, H. Yi, B. S. Li, R. Deng, S. Y. Liu and Y. J. Zhang, Recent advances in sensors for tetracycline antibiotics and their applications, *TrAC, Trends Anal. Chem.*, 2018, **109**, 260–274.
62 R. Daghrir and P. Drogui, Tetracycline antibiotics in the environment: a review, *Environ. Chem. Lett.*, 2013, **11**, 209–227.
63 T. H. Grossman, Tetracycline antibiotics and resistance, *Cold Spring Harbor Perspect. Med.*, 2016, **6**, 1–24.
64 M. L. Nelson, The chemistry and biology of the tetracyclines, *Annu. Rep. Med. Chem.*, 2002, **37**, 105–114.
65 B. R. Rifkin, A. T. Vernillo, L. M. Golub and N. S. Ramamurthy, Modulation of bone-resorption by tetracyclines, *Ann. N. Y. Acad. Sci.*, 1994, **732**, 165–180.
66 D. Vitorovic, Z. Nikolic and D. Cvetkovic, In-vivo tetracycline labeling as a measure of rearing-system influence on chicken-bone dynamics, *Zentralbl. Veterinaermed., Reihe C*, 1995, **24**, 85–86.
67 R. A. Milch, D. P. Rall and J. E. Tobie, Bone localization of the tetracyclines, *J. Natl. Cancer Inst.*, 1957, **19**, 87–93.
68 C. Pautke, F. Bauer, O. Bissinger, T. Tischer, K. Kreutzer, T. Steiner, J. Weitz, S. Otto, K. D. Wolff, S. R. Sturzenbaum and A. Kolk, Tetracycline bone fluorescence: a valuable marker for osteonecrosis characterization and therapy, *J. Oral. Maxil. Surg.*, 2010, **68**, 125–129.
69 C. S. Tam and W. Anderson, Tetracycline labeling of bone in vivo, *Calcif. Tissue Int.*, 1980, **30**, 121–125.
70 J. S. Jung, D. Jo, G. Jo and H. Hyun, Near-infrared iontrast agents for bone-targeted imaging, *Tissue Eng. Regener. Med.*, 2019, **16**, 443–450.
71 K. H. Ibsen and M. R. Urist, The biochemistry and the physiology of the tetracyclines: with special reference to mineralized tissues, *Clin. Orthop. Relat. Res.*, 1964, **32**, 143–169.
72 A. Albert and C. W. Rees, Avidity of the tetracyclines for the cations of metals, *Nature*, 1956, **177**, 433–434.
73 M. I. Kay, R. A. Young and A. S. Posner, Crystal structure of hydroxyapatite, *Nature*, 1964, **204**, 1050–1052.
74 H. C. W. Skinner and J. Nalbandian, Tetracyclines and mineralized tissues – review and perspectives, *Yale J. Biol. Med.*, 1975, **48**, 377–397.
75 Y. Kim, J. Kim, H. Lee, W. R. Shin, S. Lee, J. Lee, J. I. Park, B. H. Jhun, Y. H. Kim, S. J. Yi and K. Kim, Tetracycline analogs inhibit osteoclast differentiation by suppressing MMP-9-mediated histone H3 cleavage, *Int. J. Mol. Sci.*, 2019, **20**, 4038.
76 C. K. Tokuhara, M. R. Santesso, G. S. N. de Oliveira, T. M. D. Ventura, J. T. Doyama, W. F. Zambuzzi and R. C. de Oliveira, Updating the role of matrix metalloproteinases in mineralized tissue and related diseases, *J. Appl. Oral Sci.*, 2019, **27**, e20180596.
77 N. Duewelhenke, O. Krut and P. Eysel, Influence on mitochondria and cytotoxicity of different antibiotics administered in high concentrations on primary human osteoblasts and cell lines, *Antimicrob. Agents Chemother.*, 2007, **51**, 54–63.
78 S. M. Almazin, R. Dziak, S. Andreana and S. G. Ciancio, The effect of doxycycline hyclate, chlorhexidine gluconate, and minocycline hydrochloride on osteoblastic proliferation and differentiation in vitro, *J. Periodontol.*, 2009, **80**, 999–1005.
79 G. Gonzalez-Avila, B. Sommer, D. A. Mendoza-Posada, C. Ramos, A. A. Garcia-Hernandez and R. Falfan-Valencia, Matrix metalloproteinases participation in the metastatic process and their diagnostic and therapeutic applications in cancer, *Crit. Rev. Oncol. Hemat.*, 2019, **137**, 57–83.
80 Y. S. Li, Q. Liu, J. Tian, H. B. He and W. Luo, Angiogenesis process in osteosarcoma: an updated perspective of pathophysiology and therapeutics, *Am. J. Med. Sci.*, 2019, **357**, 280–288.
81 N. Cui, M. Hu and R. A. Khalil, Biochemical and biological attributes of matrix metalloproteinases, *Prog. Mol. Biol. Transl. Sci.*, 2017, **147**, 1–73.
82 R. S. Fife, G. W. Sledge, S. Sissons and B. Zerler, Effects of tetracyclines on angiogenesis *in vitro*, *Cancer Lett.*, 2000, **153**, 75–78.
83 A. C. Hadjimichael, A. F. Foukas, O. D. Savvidou, A. F. Mavrogenis, A. K. Psyrri and P. J. Papagelopoulos, The anti-neoplastic effect of doxycycline in osteosarcoma as a metalloproteinase (MMP) inhibitor: a systematic review, *Clin. Sarcoma Res.*, 2020, **10**, 7.
84 Z. Saikali and G. Singh, Doxycycline and other tetracyclines in the treatment of bone metastasis, *Anticancer Drugs*, 2003, **14**, 773–778.
85 M. L. Zoch, T. L. Clemens and R. C. Riddle, New insights into the biology of osteocalcin, *Bone*, 2016, **82**, 42–49.
86 M. A. Icer and M. Gezmen-Karadag, The multiple functions and mechanisms of osteopontin, *Clin. Biochem.*, 2018, **59**, 17–24.
87 H. Ritchie, The functional significance of dentin sialoprotein-phosphophoryn and dentin sialoprotein, *Int. J. Oral Sci.*, 2018, **10**, 31.
88 A. Neve, A. Corrado and F. P. Cantatore, Osteocalcin: skeletal and extra-skeletal effects, *J. Cell. Physiol.*, 2013, **228**, 1149–1153.
89 B. Ganss, R. H. Kim and J. Sodek, Bone sialoprotein, *Crit. Rev. Oral Biol. Med.*, 1999, **10**, 79–98.
90 R. Fujisawa and Y. Kuboki, Preferential adsorption of dentin and bone acidic proteins on the (100) face of hydroxyapatite crystals, *Biochim. Biophys. Acta*, 1991, **1075**, 56–60.
91 S. Kasugai, R. Fujisawa, Y. Waki, K. Miyamoto and K. Ohya, Selective drug delivery system to bone: Small peptide (Asp)(6) conjugation, *J. Bone Miner. Res.*, 2000, **15**, 936–943.
92 T. Nakato, M. Yoshitake, K. Matsubara, M. Tomida and T. Kakuchi, Relationships between structure and properties of poly(aspartic acid)s, *Macromolecules*, 1998, **31**, 2107–2113.

93 A. Bennick, M. Cannon and G. Madapallimattam, Nature of the hydroxyapatite-binding site in salivary acidic proline-rich proteins, *Biochem. J.*, 1979, **183**, 115–126.
94 D. K. Yarbrough, E. Hagerman, R. Eckert, J. He, H. Choi, N. Cao, K. Le, J. Hedger, F. X. Qi, M. Anderson, B. Rutherford, B. Wu, S. Tetradis and W. Y. Shi, Specific binding and mineralization of calcified surfaces by small peptides, *Calcif. Tissue Int.*, 2010, **86**, 58–66.
95 E. J. Carbone, K. Rajpura, B. N. Allen, E. Cheng, B. D. Ulery and K. W. H. Lo, Osteotropic nanoscale drug delivery systems based on small molecule bone-targeting moieties, *Nanomedicine*, 2017, **13**, 37–47.
96 D. Wang, S. C. Miller, L. S. Shlyakhtenko, A. M. Portillo, X. M. Liu, K. Papangkorn, P. Kopekova, Y. Lyubchenko, W. I. Higuchi and J. Kopecek, Osteotropic peptide that differentiates functional domains of the skeleton, *Bioconjugate Chem.*, 2007, **18**, 1375–1378.
97 G. Zhang, B. S. Guo, H. Wu, T. Tang, B. T. Zhang, L. Z. Zheng, Y. X. He, Z. J. Yang, X. H. Pan, H. Chow, K. To, Y. P. Li, D. H. Li, X. L. Wang, Y. X. Wang, K. Lee, Z. B. Hou, N. Dong, G. Li, K. Leung, L. Hung, F. C. He, L. Q. Zhang and L. Qin, A delivery system targeting bone formation surfaces to facilitate RNAi-based anabolic therapy, *Nat. Med.*, 2012, **18**, 307–314.
98 D. Wang, S. C. Miller, P. Kopeckova and J. Kopecek, Bone-targeting macromolecular therapeutics, *Adv. Drug Delivery Rev.*, 2005, **57**, 1049–1076.
99 Y. Sun, X. Z. Ye, M. X. Cai, X. N. Liu, J. Xiao, C. Y. Zhang, Y. Y. Wang, L. Yang, J. F. Liu, S. N. Li, C. Kang, B. Zhang, Q. Zhang, Z. L. Wang, A. Hong and X. G. Wang, Osteoblast-targeting-peptide modified nanoparticle for siRNA/microRNA delivery, *ACS Nano*, 2016, **10**, 5759–5768.
100 S. J. Segvich, H. C. Smith and D. H. Kohn, The adsorption of preferential binding peptides to apatite-based materials, *Biomaterials*, 2009, **30**, 1287–1298.
101 W. N. Addison, S. J. Miller, J. Ramaswamy, A. Mansouri, D. H. Kohn and M. D. Mckee, Phosphorylation-dependent mineral-type specificity for apatite-binding peptide sequences, *Biomaterials*, 2010, **31**, 9422–9430.
102 C. Ling, W. L. Zhao, Z. Q. Wang, J. D. Chen, P. Ustriyana, M. Gao and N. Sahai, Structure-activity relationships of hydroxyapatite-binding peptides, *Langmuir*, 2020, **36**, 2729–2739.
103 A. K. Bassi, J. E. Gough, M. Zakikhani and S. Downes, The chemical and physical properties of poly(epsilon-caprolactone) scaffolds functionalised with poly(vinyl phosphonic acid-co-acrylic acid), *J. Tissue Eng.*, 2011, **2011**, 615328.
104 A. K. Ghag, J. E. Gough and S. Downes, The osteoblast and osteoclast responses to phosphonic acid containing poly(epsilon-caprolactone) electrospun scaffolds, *Biomater. Sci.*, 2014, **2**, 233–241.
105 A. Akbarzadeh, R. Rezaei-Sadabady, S. Davaran, S. W. Joo, N. Zarghami, Y. Hanifehpour, M. Samiei, M. Kouhi and K. Nejati-Koshki, Liposome: classification, preparation, and applications, *Nanoscale Res. Lett.*, 2013, **8**, 102.
106 G. Amoabediny, F. Haghiralsadat, S. Naderinezhad, M. N. Helder, E. A. Kharanaghi, J. M. Arough and B. Zandieh-Doulabi, Overview of preparation methods of polymeric and lipid-based (niosome, solid lipid, liposome) nanoparticles: a comprehensive review, *Int. J. Polym. Mater. Polym. Biomater.*, 2018, **67**, 383–400.
107 D. Lombardo, P. Calandra, D. Barreca, S. Magazu and M. A. Kiselev, Soft interaction in liposome nanocarriers for therapeutic drug delivery, *Nanomaterials*, 2016, **6**, 125.
108 S. Z. Vahed, R. Salehi, S. Davaran and S. Sharifi, Liposome-based drug co-delivery systems in cancer cells, *Mater. Sci. Eng., C*, 2017, **71**, 1327–1341.
109 K. S. Ahmed, S. A. Hussein, A. H. Ali, S. A. Korma, L. P. Qiu and J. H. Chen, Liposome: composition, characterisation, preparation, and recent innovation in clinical applications, *J. Drug Targeting*, 2019, **27**, 742–761.
110 N. Filipczak, J. Y. Pan, S. S. K. Yalamarty and V. P. Torchilin, Recent advancements in liposome technology, *Adv. Drug Delivery Rev.*, 2020, **156**, 4–22.
111 S. Yamashita, H. Katsumi, N. Hibino, Y. Isobe, Y. Yagi, Y. Tanaka, S. Yamada, C. Naito and A. Yamamoto, Development of PEGylated aspartic acid-modified liposome as a bone-targeting carrier for the delivery of paclitaxel and treatment of bone metastasis, *Biomaterials*, 2018, **154**, 74–85.
112 F. H. Meng, Z. Y. Zhong and J. Feijen, Stimuli-responsive polymersomes for programmed drug delivery, *Biomacromolecules*, 2009, **10**, 197–209.
113 F. Y. K. Wang, J. G. Xiao, S. Chen, H. Sun, B. Yang, J. H. Jiang, X. Zhou and J. Z. Du, Polymer vesicles: modular platforms for cancer theranostics, *Adv. Mater.*, 2018, **30**, 1705674.
114 E. G. Bellomo, M. D. Wyrsta, L. Pakstis, D. J. Pochan and T. J. Deming, Stimuli-responsive polypeptide vesicles by conformation-specific assembly, *Nat. Mater.*, 2004, **3**, 244–248.
115 J. Z. Du and R. K. O'Reilly, Advances and challenges in smart and functional polymer vesicles, *Soft Matter*, 2009, **5**, 3544–3561.
116 D. E. Discher and A. Eisenberg, Polymer vesicles, *Science*, 2002, **297**, 967–973.
117 P. Tanner, P. Baumann, R. Enea, O. Onaca, C. Palivan and W. Meier, Polymeric vesicles: from drug carriers to nanoreactors and artificial organelles, *Acc. Chem. Res.*, 2011, **44**, 1039–1049.
118 P. Broz, S. M. Benito, C. Saw, P. Burger, H. Heider, M. Pfisterer, S. Marsch, W. Meier and P. Hunziker, Cell targeting by a generic receptor-targeted polymer nanocontainer platform, *J. Controlled Release*, 2005, **102**, 475–488.
119 H. Sun, D. Q. Liu and J. Z. Du, Nanobowls with controlled openings and interior holes driven by the synergy of hydrogen bonding and π-π interaction, *Chem. Sci.*, 2019, **10**, 657–664.
120 J. G. Xiao and J. Z. Du, Tetrapod Polymersomes, *J. Am. Chem. Soc.*, 2020, **142**, 6569–6577.
121 S. K. Lim, A. S. W. Wong, H. P. M. de Hoog, P. Rangamani, A. N. Parikh, M. Nallani, S. Sandin and B. Liedberg,

Spontaneous formation of nanometer scale tubular vesicles in aqueous mixtures of lipid and block copolymer amphiphiles, *Soft Matter*, 2017, **13**, 1107–1115.

122 J. R. Chen, N. E. Clay, N. H. Park and H. Kong, Non-spherical particles for targeted drug delivery, *Chem. Eng. Sci.*, 2015, **125**, 20–24.

123 Y. M. Chen, J. Z. Du, M. Xiong, H. X. Guo, H. Jinnai and T. Kaneko, Perforated block copolymer vesicles with a highly folded membrane, *Macromolecules*, 2007, **40**, 4389–4392.

124 Y. Morishima, Thermally responsive polymer vesicles, *Angew. Chem., Int. Ed.*, 2007, **46**, 1370–1372.

125 Y. Q. Zhu, B. Yang, S. Chen and J. Z. Du, Polymer vesicles: Mechanism, preparation, application, and responsive behavior, *Prog. Polym. Sci.*, 2017, **64**, 1–22.

126 J. H. Jiang, X. Y. Zhang, Z. Fan and J. Z. Du, Ring-opening polymerization of N-carboxyanhydride-induced self-assembly for fabricating biodegradable polymer vesicles, *ACS Macro Lett.*, 2019, **8**, 1216–1221.

127 Z. H. Lu and J. S. Guo, Growing polymer vesicles generated by polymerization induced self-assembly coupled with a living chemical reactor, *Front. Bioeng. Biotechnol.*, 2020, **8**, 1018.

128 P. J. Docherty, C. Girou, M. J. Derry and S. P. Armes, Epoxy-functional diblock copolymer spheres, worms and vesicles via polymerization-induced self-assembly in mineral oil, *Polym. Chem.*, 2020, **11**, 3332–3339.

129 X. Zhou, N. Yan, E. J. Cornel, H. D. Cai, S. B. Xue, H. Xi, Z. Fan, S. S. He and J. Z. Du, Bone-targeting polymer vesicles for simultaneous imaging and effective malignant bone tumor treatment, *Biomaterials*, 2021, **269**, 120345.

130 K. Kataoka, A. Harada and Y. Nagasaki, Block copolymer micelles for drug delivery: Design, characterization and biological significance, *Adv. Drug Delivery Rev.*, 2012, **64**, 37–48.

131 G. Giorgio, G. Colafemmina, F. Mavelli, S. Murgia and G. Palazzo, The impact of alkanes on the structure of Triton X100 micelles, *RSC Adv.*, 2016, **6**, 825–836.

132 G. S. Kwon and T. Okano, Polymeric micelles as new drug carriers, *Adv. Drug Delivery Rev.*, 1996, **21**, 107–116.

133 V. P. Torchilin, Micellar nanocarriers: Pharmaceutical perspectives, *Pharm. Res.*, 2007, **24**, 1–16.

134 N. A. N. Hanafy, M. El-Kemary and S. Leporatti, Micelles structure development as a strategy to improve smart cancer therapy, *Cancers*, 2018, **10**, 238.

135 A. Mandal, R. Bisht, I. D. Rupenthal and A. K. Mitra, Polymeric micelles for ocular drug delivery: from structural frameworks to recent preclinical studies, *J. Controlled Release*, 2017, **248**, 96–116.

136 Y. S. Wang, G. L. Li, S. B. Zhu, F. C. Jing, R. D. Liu, S. S. Li, J. He and J. D. Lei, A self-assembled nanoparticle platform based on amphiphilic oleanolic acid polyprodrug for cancer therapy, *Chin, J. Polym. Sci.*, 2020, **38**, 819–829.

137 Y. H. Xie, C. C. Liu, H. W. Huang, J. Huang, A. P. Deng, P. Zou and X. Y. Tan, Bone-targeted delivery of simvastatin-loaded PEG-PLGA micelles conjugated with tetracycline for osteoporosis treatment, *Drug Delivery Transl. Res.*, 2018, **8**, 1090–1102.

138 J. H. Zhu, Q. Huo, M. Xu, F. Yang, Y. Li, H. H. Shi, Y. M. Niu and Y. Liu, Bortezomib-catechol conjugated prodrug micelles: combining bone targeting and aryl boronate-based pH-responsive drug release for cancer bone-metastasis therapy, *Nanoscale*, 2018, **10**, 18387–18397.

139 J. M. Anderson and M. S. Shive, Biodegradation and biocompatibility of PLA and PLGA microspheres, *Adv. Drug Delivery Rev.*, 2012, **64**, 72–82.

140 S. Acharya and S. K. Sahoo, PLGA nanoparticles containing various anticancer agents and tumour delivery by EPR effect, *Adv. Drug Delivery Rev.*, 2011, **63**, 170–183.

141 C. E. Astete and C. M. Sabliov, Synthesis and characterization of PLGA nanoparticles, *J. Biomater. Sci., Polym. Ed.*, 2006, **17**, 247–289.

142 S. I. Thamake, S. L. Raut, Z. Gryczynski, A. P. Ranjan and J. K. Vishwanatha, Alendronate coated poly-lactic-co-glycolic acid (PLGA) nanoparticles for active targeting of metastatic breast cancer, *Biomaterials*, 2012, **33**, 7164–7173.

143 H. Wang, J. Liu, S. Tao, G. H. Chai, J. W. Wang, F. Q. Hu and H. Yuan, Tetracycline-grafted PLGA nanoparticles as bone-targeting drug delivery system, *Int. J. Nanomed.*, 2015, **10**, 5671–5685.

144 P. Agrawal, G. J. Strijkers and K. Nicolay, Chitosan-based systems for molecular imaging, *Adv. Drug Delivery Rev.*, 2010, **62**, 42–58.

145 K. Y. Lee, J. H. Kim, I. C. Kwon and S. Y. Jeong, Self-aggregates of deoxycholic acid modified chitosan as a novel carrier of adriamycin, *Colloid Polym. Sci.*, 2000, **278**, 1216–1219.

146 E. Ruel-Gariepy, G. Leclair, P. Hildgen, A. Gupta and J. C. Leroux, Thermosensitive chitosan-based hydrogel containing liposomes for the delivery of hydrophilic molecules, *J. Controlled Release*, 2002, **82**, 373–383.

147 S. Hein, K. Wang, W. F. Stevens and J. Kjems, Chitosan composites for biomedical applications: status, challenges and perspectives, *Mater. Sci. Technol.*, 2008, **24**, 1053–1061.

148 H. M. Yi, L. Q. Wu, W. E. Bentley, R. Ghodssi, G. W. Rubloff, J. N. Culver and G. F. Payne, Biofabrication with chitosan, *Biomacromolecules*, 2005, **6**, 2881–2894.

149 Y. Yang, S. P. Wang, Y. T. Wang, X. H. Wang, Q. Wang and M. W. Chen, Advances in self-assembled chitosan nanomaterials for drug delivery, *Biotechnol. Adv.*, 2014, **32**, 1301–1316.

150 A. Rampino, M. Borgogna, P. Blasi, B. Bellich and A. Cesaro, Chitosan nanoparticles: preparation, size evolution and stability, *Int. J. Pharm.*, 2013, **455**, 219–228.

151 J. P. Quinones, H. Peniche and C. Peniche, Chitosan based self-assembled nanoparticles in drug delivery, *Polymers*, 2018, **10**, 235.

152 S. Santhosh, D. Mukherjee, J. Anbu, M. Murahari and B. V. Teja, Improved treatment efficacy of risedronate functionalized chitosan nanoparticles in osteoporosis: formulation development, in vivo, and molecular modelling studies, *J. Microencapsulation*, 2019, **36**, 338–355.

153 B. Balakrishnan and A. Jayakrishnan, Self-cross-linking biopolymers as injectable in situ forming biodegradable scaffolds, *Biomaterials*, 2005, **26**, 3941–3951.
154 Y. Tabata and Y. Ikada, Protein release from gelatin matrices, *Adv. Drug Delivery Rev.*, 1998, **31**, 287–301.
155 J. Y. Lai, Biocompatibility of chemically cross-linked gelatin hydrogels for ophthalmic use, *J. Mater. Sci.: Mater. Med.*, 2010, **21**, 1899–1911.
156 S. Young, M. Wong, Y. Tabata and A. G. Mikos, Gelatin as a delivery vehicle for the controlled release of bioactive molecules, *J. Controlled Release*, 2005, **109**, 256–274.
157 Z. S. Patel, M. Yamamoto, H. Ueda, Y. Tabata and A. G. Mikos, Biodegradable gelatin microparticles as delivery systems for the controlled release of bone morphogenetic protein-2, *Acta Biomater.*, 2008, **4**, 1126–1138.
158 M. P. Ferraz, F. J. Monteiro and C. M. Manuel, Hydroxyapatite nanoparticles: a review of preparation methodologies, *J. Appl. Biomater. Biomech.*, 2004, **2**, 74–80.
159 Y. B. Qiu, X. D. Xu, W. Z. Guo, Y. Zhao, J. H. Su and J. Chen, Mesoporous hydroxyapatite nanoparticles mediate the release and bioactivity of BMP-2 for enhanced bone regeneration, *ACS Biomater. Sci. Eng.*, 2020, **6**, 2323–2335.
160 A. Barbanente, B. Palazzo, L. Degli Esposti, A. Adamiano, M. Iafisco, N. Ditaranto, D. Migoni, F. Gervaso, R. Nadar, P. Ivanchenko, S. Leeuwenburgh and N. Margiotta, Selenium-doped hydroxyapatite nanoparticles for potential application in bone tumor therapy, *J. Inorg. Biochem.*, 2021, **215**, 111334.
161 T. Song, F. X. Zhao, Y. Y. Wang, D. X. Li, N. Lei, X. F. Li, Y. M. Xiao and X. D. Zhang, Constructing a biomimetic nanocomposite with the in situ deposition of spherical hydroxyapatite nanoparticles to induce bone regeneration, *J. Mater. Chem. B*, 2021, **9**, 2469–2482.
162 L. Pasqua, I. E. De Napoli, M. De Santo, M. Greco, E. Catizzone, D. Lombardo, G. Montera, A. Comande, A. Nigro, C. Morelli and A. Leggio, Mesoporous silica-based hybrid materials for bone-specific drug delivery, *Nanoscale Adv.*, 2019, **1**, 3269–3278.
163 F. Wang, M. S. Li, Y. P. Lu and Y. X. Qi, A simple sol-gel technique for preparing hydroxyapatite nanopowders, *Mater. Lett.*, 2005, **59**, 916–919.
164 G. C. Koumoulidis, A. P. Katsoulidis, A. K. Ladavos, P. J. Pomonis, C. C. Trapalis, A. T. Sdoukos and T. C. Vaimakis, Preparation of hydroxyapatite via microemulsion route, *J. Colloid Interface Sci.*, 2003, **259**, 254–260.
165 Y. J. Wang, S. H. Zhang, K. Wei, N. R. Zhao, J. D. Chen and X. D. Wang, Hydrothermal synthesis of hydroxyapatite nanopowders using cationic surfactant as a template, *Mater. Lett.*, 2006, **60**, 1484–1487.
166 P. Parhi, A. Ramanan and A. R. Ray, A convenient route for the synthesis of hydroxyapatite through a novel microwave-mediated metathesis reaction, *Mater. Lett.*, 2004, **58**, 3610–3612.
167 Z. L. Shi, X. Huang, Y. R. Cai, R. K. Tang and D. S. Yang, Size effect of hydroxyapatite nanoparticles on proliferation and apoptosis of osteoblast-like cells, *Acta Biomater.*, 2009, **5**, 338–345.
168 J. P. Richard, K. Melikov, E. Vives, C. Ramos, B. Verbeure, M. J. Gait, L. V. Chernomordik and B. Lebleu, Cell-penetrating peptides: a reevaluation of the mechanism of cellular uptake, *J. Biol. Chem.*, 2003, **278**, 585–590.
169 S. Maeno, Y. Niki, H. Matsumoto, H. Morioka, T. Yatabe, A. Funayama, Y. Toyama, T. Taguchi and J. Tanaka, The effect of calcium ion concentration on osteoblast viability, proliferation and differentiation in monolayer and 3D culture, *Biomaterials*, 2005, **26**, 4847–4855.
170 M. Nagano, T. Nakamura, T. Kokubo, M. Tanahashi and M. Ogawa, Differences of bone bonding ability and degradation behaviour in vivo between amorphous calcium phosphate and highly crystalline hydroxyapatite coating, *Biomaterials*, 1996, **17**, 1771–1777.
171 Y. Zhao, Y. Zhang, F. Ning, D. Guo and Z. Xu, Synthesis and cellular biocompatibility of two kinds of HAP with different nanocrystal morphology, *J. Biomed. Mater. Res., Part B*, 2007, **83B**, 121–126.
172 R. Saunders, K. H. Szymczyk, I. M. Shapiro and C. S. Adams, Matrix regulation of skeletal cell apoptosis III: mechanism of ion pair-induced apoptosis, *J. Cell. Biochem.*, 2007, **100**, 703–715.
173 D. K. Khajuria, V. B. Kumar, D. Gigi, A. Gedanken and D. Karasik, Accelerated bone regeneration by nitrogen-doped carbon dots functionalized with hydroxyapatite nanoparticles, *ACS Appl. Mater. Interfaces*, 2018, **10**, 19373–19385.
174 A. L. C. Maia, C. D. Ferreira, A. L. B. de Barros, A. T. M. E. Silva, G. A. Ramaldes, A. D. Cunha, D. C. D. Oliveira, C. Fernandes and D. C. F. Soares, Vincristine-loaded hydroxyapatite nanoparticles as a potential delivery system for bone cancer therapy, *J. Drug Targeting*, 2018, **26**, 592–603.
175 M. S. Nanes, Tumor necrosis factor-alpha: molecular and cellular mechanisms in skeletal pathology, *Gene*, 2003, **321**, 1–15.
176 B. F. Boyce, Z. Q. Yao and L. P. Xing, Functions of nuclear factor kappa B in bone, *Ann. N. Y. Acad. Sci.*, 2010, **1192**, 367–375.
177 J. Lu, M. Liong, J. I. Zink and F. Tamanoi, Mesoporous silica nanoparticles as a delivery system for hydrophobic anticancer drugs, *Small*, 2007, **3**, 1341–1346.
178 J. L. Paris and M. Vallet-Regi, Mesoporous silica nanoparticles for co-delivery of drugs and nucleic acids in oncology: a review, *Pharmaceutics*, 2020, **12**, 526.
179 E. D. M. Isa, H. Ahmad, M. B. A. Rahman and M. R. Gill, Progress in mesoporous silica nanoparticles as drug delivery agents for cancer treatment, *Pharmaceutics*, 2021, **13**, 152.
180 I. I. Slowing, B. G. Trewyn, S. Giri and V. S. Y. Lin, Mesoporous silica nanoparticles for drug delivery and biosensing applications, *Adv. Funct. Mater.*, 2007, **17**, 1225–1236.
181 M. Manzano and M. Vallet-Regi, Mesoporous silica nanoparticles for drug delivery, *Adv. Funct. Mater.*, 2020, **30**, 1902634.
182 M. Vallet-Regi, M. Colilla, I. Izquierdo-Barba and M. Manzano, Mesoporous silica nanoparticles for drug delivery: current insights, *Molecules*, 2018, **23**, 47.

183 Y. X. Zhou, G. L. Quan, Q. L. Wu, X. X. Zhang, B. Y. Niu, B. Y. Wu, Y. Huang, X. Pan and C. B. Wu, Mesoporous silica nanoparticles for drug and gene delivery, *Acta Pharm. Sin. B*, 2018, **8**, 165–177.

184 X. H. Pu, J. Li, P. Qiao, M. M. Li, H. Y. Wang, L. L. Zong, Q. Yuan and S. F. Duan, Mesoporous silica nanoparticles as a prospective and promising approach for drug delivery and biomedical applications, *Curr. Cancer Drug Targets*, 2019, **19**, 285–295.

185 J. J. Liu, Z. Luo, J. X. Zhang, T. T. Luo, J. Zhou, X. J. Zhao and K. Y. Cai, Hollow mesoporous silica nanoparticles facilitated drug delivery via cascade pH stimuli in tumor microenvironment for tumor therapy, *Biomaterials*, 2016, **83**, 51–65.

186 Y. Alyassin, E. G. Sayed, P. Mehta, K. Ruparelia, M. S. Arshad, M. Rasekh, J. Shepherd, I. Kucuk, P. B. Wilson, N. Singh, M. W. Chang, D. G. Fatouros and Z. Ahmad, Application of mesoporous silica nanoparticles as drug delivery carriers for chemotherapeutic agents, *Drug Discovery Today*, 2020, **25**, 1513–1520.

187 C. Y. Lai, B. G. Trewyn, D. M. Jeftinija, K. Jeftinija, S. Xu, S. Jeftinija and V. S. Y. Lin, A mesoporous silica nanosphere-based carrier system with chemically removable CdS nanoparticle caps for stimuli-responsive controlled release of neurotransmitters and drug molecules, *J. Am. Chem. Soc.*, 2003, **125**, 4451–4459.

188 C. E. Fowler, D. Khushalani, B. Lebeau and S. Mann, Nanoscale materials with mesostructured interiors, *Adv. Mater.*, 2001, **13**, 649–652.

189 R. I. Nooney, D. Thirunavukkarasu, Y. M. Chen, R. Josephs and A. E. Ostafin, Synthesis of nanoscale mesoporous silica spheres with controlled particle size, *Chem. Mater.*, 2002, **14**, 4721–4728.

190 J. G. Croissant, Y. Fatieiev and N. M. Khashab, Degradability and clearance of silicon, organosilica, silsesquioxane, silica mixed oxide, and mesoporous silica nanoparticles, *Adv. Mater.*, 2017, **29**, 1604634.

191 N. Z. Knezevic and J. O. Durand, Large pore mesoporous silica nanomaterials for application in delivery of biomolecules, *Nanoscale*, 2015, **7**, 2199–2209.

192 S. M. Egger, K. R. Hurley, A. Datt, G. Swindlehurst and C. L. Haynes, Ultraporous mesostructured silica nanoparticles, *Chem. Mater.*, 2015, **27**, 3193–3196.

193 F. Hoffmann, M. Cornelius, J. Morell and M. Froba, Silica-based mesoporous organic-inorganic hybrid materials, *Angew. Chem., Int. Ed.*, 2006, **45**, 3216–3251.

194 W. T. Sun, K. Ge, Y. Jin, Y. Han, H. S. Zhang, G. Q. Zhou, X. J. Yang, D. D. Liu, H. F. Liu, X. J. Liang and J. C. Zhang, Bone-targeted nanoplatform combining zoledronate and photothermal therapy to treat breast cancer bone metastasis, *ACS Nano*, 2019, **13**, 7556–7567.

195 Y. Li, D. W. Ye, M. X. Li, M. Ma and N. Gu, Adaptive materials based on iron oxide nanoparticles for bone regeneration, *ChemPhysChem*, 2018, **19**, 1965–1979.

196 D. Bobo, K. J. Robinson, J. Islam and K. J. Thurecht, and S. R. Corrie, Nanoparticle-based medicines: a review of FDA-approved materials and clinical trials to date, *Pharm. Res.*, 2016, **33**, 2373–2387.

197 M. R. Bashir, L. Bhatti, D. Marin and R. C. Nelson, Emerging applications for ferumoxytol as a contrast agent in MRI, *J. Magn. Reson. Imaging*, 2015, **41**, 884–898.

198 C. C. Berry and A. S. G. Curtis, Functionalisation of magnetic nanoparticles for applications in biomedicine, *J. Phys. D: Appl. Phys.*, 2003, **36**, R198–R206.

199 O. Veiseh, J. W. Gunn and M. Q. Zhang, Design and fabrication of magnetic nanoparticles for targeted drug delivery and imaging, *Adv. Drug Delivery Rev.*, 2010, **62**, 284–304.

200 K. Kannan, J. Mukherjee and M. N. Gupta, Use of polyethyleneimine coated Fe_3O_4 nanoparticles as an ion-exchanger for protein separation, *Sci. Adv. Mater.*, 2013, **5**, 1477–1484.

201 S. Yang, X. Zhang, W. T. Zhao, L. Q. Sun and A. Q. Luo, Preparation and evaluation of Fe_3O_4 nanoparticles incorporated molecularly imprinted polymers for protein separation, *J. Mater. Sci.*, 2016, **51**, 937–949.

202 H. W. Gu, K. M. Xu, C. J. Xu and B. Xu, Biofunctional magnetic nanoparticles for protein separation and pathogen detection, *Chem. Commun.*, 2006, 941–949.

203 R. Y. Hong, J. H. Li, S. Z. Zhang, H. Z. Li, Y. Zheng, J. M. Ding and D. G. Wei, Preparation and characterization of silica-coated Fe_3O_4 nanoparticles used as precursor of ferrofluids, *Appl. Surf. Sci.*, 2009, **255**, 3485–3492.

204 R. A. Pareta, E. Taylor and T. J. Webster, Increased osteoblast density in the presence of novel calcium phosphate coated magnetic nanoparticles, *Nanotechnology*, 2008, **19**, 265101.

205 B. Brocklehurst, Magnetic fields and radical reactions: recent developments and their role in nature, *Chem. Soc. Rev.*, 2002, **31**, 301–311.

206 R. H. W. Funk, T. Monsees and N. Ozkucur, Electromagnetic effects – From cell biology to medicine, *Prog. Histochem. Cytochem.*, 2009, **43**, 177–264.

207 A. Panahifar, M. Mahmoudi and M. R. Doschak, Synthesis and in vitro evaluation of bone-seeking superparamagnetic iron oxide nanoparticles as contrast agents for imaging bone metabolic activity, *ACS Appl. Mater. Interfaces*, 2013, **5**, 5219–5226.

208 M. S. Lee, C. M. Su, J. C. Yeh, P. R. Wu, T. Y. Tsai and S. L. Lou, Synthesis of composite magnetic nanoparticles Fe_3O_4 with alendronate for osteoporosis treatment, *Int. J. Nanomed.*, 2016, **11**, 4583–4594.

209 K. S. Brammer, C. J. Frandsen and S. Jin, TiO_2 nanotubes for bone regeneration, *Trends Biotechnol.*, 2012, **30**, 315–322.

210 K. S. Brammer, S. Oh, C. J. Cobb, L. M. Bjursten, H. van der Heyde and S. Jin, Improved bone-forming functionality on diameter-controlled TiO_2 nanotube surface, *Acta Biomater.*, 2009, **5**, 3215–3223.

211 K. Zazakowny, J. Lewandowska-Lancucka, J. Mastalska-Poplawska, K. Kaminski, A. Kusior, M. Radecka and M. Nowakowska, Biopolymeric hydrogels – nanostructured

TiO_2 hybrid materials as potential injectable scaffolds for bone regeneration, *Colloids Surf., B*, 2016, **148**, 607–614.

212 R. Ikono, N. Li, N. H. Pratama, A. Vibriani, D. R. Yuniarni, M. Luthfansyah, B. M. Bachtiar, E. W. Bachtiar, K. Mulia, M. Nasikin, H. Kagami, X. Li, E. Mardliyati, N. T. Rochman, T. Nagamura-Inoue and A. Tojo, Enhanced bone regeneration capability of chitosan sponge coated with TiO_2 nanoparticles, *Biotechnol. Rep.*, 2019, **24**, e00350.

213 J. D. Sun, Y. Zhu, L. Meng, W. Wei, Y. Li, X. Y. Liu and Y. F. Zheng, Controlled release and corrosion protection by self-assembled colloidal particles electrodeposited onto magnesium alloys, *J. Mater. Chem. B*, 2015, **3**, 1667–1676.

214 Y. Li, L. Liu, X. Qu, L. Ren and K. Dai, Drug delivery property, antibacterial performance and cytocompatibility of gentamicin loaded poly(lactic-co-glycolic acid) coating on porous magnesium scaffold, *Mater. Technol.*, 2015, **30**, B96–B103.

215 C. Y. Li, Y. J. Zhang, G. C. Chen, F. Hu, K. Zhao and Q. B. Wang, Engineered multifunctional nanomedicine for simultaneous stereotactic chemotherapy and inhibited osteolysis in an orthotopic model of bone metastasis, *Adv. Mater.*, 2017, **29**, 895–903.

216 X. Yang, X. An, S. Ling, H. Huang, Y. Zhang, G. Chen, C. Li and Q. Wang, A cascade targeted and activatable NIR-II nanoprobe for highly sensitive detection of acute myeloid leukemia in an orthotopic model, *CCS Chem.*, 2021, **3**, 895–903.

217 L. L. Tan, X. M. Yu, P. Wan and K. Yang, Biodegradable materials for bone repairs: a review, *J. Mater. Sci. Technol.*, 2013, **29**, 503–513.

218 M. Hameed and H. Dorfman, Primary malignant bone tumors-recent developments, *Semin. Diagn. Pathol.*, 2011, **28**, 86–101.

219 K. Berner, T. B. Johannesen, A. Berner, H. K. Haugland, B. Bjerkehagen, P. J. Bohler and O. S. Bruland, Time-trends on incidence and survival in a nationwide and unselected cohort of patients with skeletal osteosarcoma, *Acta Oncol.*, 2015, **54**, 25–33.

220 E. Simpson and H. L. Brown, Understanding osteosarcomas, *JAAPA – J. Am. Acad. Phys.*, 2018, **31**, 15–19.

221 L. C. Hofbauer, T. D. Rachner, R. E. Coleman and F. Jakob, Endocrine aspects of bone metastases, *Lancet Diabetes Endocrinol.*, 2014, **2**, 500–512.

222 L. J. Suva, C. Washam, R. W. Nicholas and R. J. Griffin, Bone metastasis: mechanisms and therapeutic opportunities, *Nat. Rev. Endocrinol.*, 2011, **7**, 208–218.

223 P. I. Croucher, M. M. McDonald and T. J. Martin, Bone metastasis: the importance of the neighbourhood, *Nat. Rev. Cancer*, 2016, **16**, 373–386.

224 G. A. Rodan and T. J. Martin, Therapeutic approaches to bone diseases, *Science*, 2000, **289**, 1508–1514.

225 R. E. Coleman, Prevention and treatment of bone metastases, *Nat. Rev. Clin. Oncol.*, 2012, **9**, 76–78.

226 R. Vinay and V. KusumDevi, Potential of targeted drug delivery system for the treatment of bone metastasis, *Drug Delivery*, 2016, **23**, 21–29.

227 J. Vanderburgh, J. L. Hill, M. K. Gupta, K. A. Kwakwa, S. K. Wang, K. Moyer, S. K. Bedingfield, A. R. Merkel, R. d'Arcy, S. A. Guelcher, J. A. Rhoades and C. L. Duvall, Tuning ligand density to optimize pharmacokinetics of targeted nanoparticles for dual protection against tumor-induced bone destruction, *ACS Nano*, 2020, **14**, 311–327.

228 M. P. di Magliano and M. Hebrok, Hedgehog signalling in cancer formation and maintenance, *Nat. Rev. Cancer*, 2003, **3**, 903–911.

229 J. Briscoe and P. P. Therond, The mechanisms of Hedgehog signalling and its roles in development and disease, *Nat. Rev. Mol. Cell Biol.*, 2013, **14**, 416–429.

230 C. B. He, Y. P. Hu, L. C. Yin, C. Tang and C. H. Yin, Effects of particle size and surface charge on cellular uptake and biodistribution of polymeric nanoparticles, *Biomaterials*, 2010, **31**, 3657–3666.

231 H. Qiao, Z. W. Cui, S. B. Yang, D. K. Ji, Y. G. Wang, Y. Yang, X. G. Han, Q. M. Fan, A. Qin, T. Y. Wang, X. P. He, W. B. Bu and T. T. Tanet, Targeting osteocytes to attenuate early breast cancer bone metastasis by theranostic upconversion nanoparticles with responsive plumbagin release, *ACS Nano*, 2017, **11**, 7259–7273.

232 W. P. Fan, W. B. Bu and J. L. Shi, On the latest three-stage development of nanomedicines based on upconversion nanoparticles, *Adv. Mater.*, 2016, **28**, 3987–4011.

233 B. L. Riggs and L. J. Melton, The worldwide problem of osteoporosis – insights afforded by epidemiology, *Bone*, 1995, **17**, S505–S511.

234 O. Johnell and J. A. Kanis, An estimate of the worldwide prevalence and disability associated with osteoporotic fractures, *Osteoporosis Int.*, 2006, **17**, 1726–1733.

235 J. A. Kanis, L. Alexeeva, J. P. Bonjour, P. Burkhardt, C. Christiansen, C. Cooper, P. Delmas, O. Johnell, C. Johnston, J. A. Kanis, N. Khaltaev, P. Lips, G. Mazzuoli, L. J. Melton, P. Meunier, E. Seeman, J. Stepan and A. Tosteson, Assessment of fracture risk and its application to screening for postmenopausal osteoporosis – synopsis of a WHO report, *Osteoporosis Int.*, 1994, **4**, 368–381.

236 J. A. Kanis, C. C. Gluer and C. S. A. I. Osteoporosis, An update on the diagnosis and assessment of osteoporosis with densitometry, *Osteoporosis Int.*, 2000, **11**, 192–202.

237 A. Unnanuntana, B. P. Gladnick, E. Donnelly and J. M. Lane, The assessment of fracture risk, *J. Bone Jt. Surg., Am. Vol.*, 2010, **92A**, 743–753.

238 J. R. Center, T. V. Nguyen, D. Schneider, P. N. Sambrook and J. A. Eisman, Mortality after all major types of osteoporotic fracture in men and women: an observational study, *Lancet*, 1999, **353**, 878–882.

239 S. R. Cummings, D. Bates and D. M. Black, Clinical use of bone densitometry – Scientific review, *JAMA, J. Am. Med. Assoc.*, 2002, **288**, 1889–1897.

240 R. M. D. Zebaze, A. Ghasem-Zadeh, A. Bohte, S. Iuliano-Burns, M. Mirams, R. I. Price, E. J. Mackie and E. Seeman, Intracortical remodelling and porosity in the distal radius and post-mortem femurs of women: a cross-sectional study, *Lancet*, 2010, **375**, 1729–1736.

241 J. Barnsley, G. Buckland, P. E. Chan, A. Ong, A. S. Ramos, M. Baxter, F. Laskou, E. M. Dennison, C. Cooper and H. P. Patel, Pathophysiology and treatment of osteoporosis: challenges for clinical practice in older people, *Aging: Clin. Exp. Res.*, 2021, **33**, 759–773.

242 Q. Y. Wang, N. Ding, Y. H. Dong, Z. X. Wen, R. Chen, S. Y. Liu, H. Liu, Z. F. Sheng and Y. N. Ou, Pharmacological treatment of osteoporosis in elderly people: a systematic review and meta-analysis, *Gerontology*, 2021, **6**, 1–11.

243 S. J. Gallacher and T. Dixon, Impact of treatments for postmenopausal osteoporosis (bisphosphonates, parathyroid hormone, strontium ranelate, and denosumab) on bone quality: a systematic review, *Calcif. Tissue Int.*, 2010, **87**, 469–484.

244 Y. Nomura, The impact of dosing frequency in compliance with bisphosphonates among postmenopausal Japanese women for osteoporosis treatment, *J. Bone Miner. Res.*, 2008, **23**, S468.

245 F. Salamanna, A. Gambardella, D. Contartese, A. Visani and M. Fini, Nano-based biomaterials as drug delivery systems against osteoporosis: a systematic review of preclinical and clinical evidence, *Nanomaterials*, 2021, **11**, 530.

246 D. L. Wei, J. S. Jung, H. L. Yang, D. A. Stout and L. Yang, Nanotechnology treatment options for osteoporosis and its corresponding consequences, *Curr. Osteoporosis Rep.*, 2016, **14**, 239–247.

247 S. Tao, S. Q. Chen, W. T. Zhou, F. Y. Yu, L. Bao, G. X. Qiu, Q. Qiao, F. Q. Hu, J. W. Wang and H. Yuan, A novel biocompatible, simvastatin-loaded, bone-targeting lipid nanocarrier for treating osteoporosis more effectively, *RSC Adv.*, 2020, **10**, 20445–20459.

248 D. J. Kotak and P. V. Devarajan, Bone targeted delivery of salmon calcitonin hydroxyapatite nanoparticles for sublingual osteoporosis therapy (SLOT), *Nanomedicine*, 2020, **24**, 102153.

249 D. S. Bilecen, J. C. Rodriguez-Cabello, H. Uludag and V. Hasirci, Construction of a PLGA based, targeted siRNA delivery system for treatment of osteoporosis, *J*, *Biomater. Sci., Polym. Ed.*, 2017, **28**, 1859–1873.

250 D. S. Bilecen, H. Uludag and V. Hasirci, Development of PEI-RANK siRNA complex loaded PLGA nanocapsules for the treatment of osteoporosis, *Tissue Eng., Part A*, 2019, **25**, 34–43.

251 J. A. Kanis, Diagnosis of osteoporosis and assessment of fracture risk, *Lancet*, 2002, **359**, 1929–1936.

252 W. Heindel, R. Gubitz, V. Vieth, M. Weckesser, O. Schober and M. Schafers, The diagnostic imaging of bone metastases, *Dtsch. Arztebl. Int.*, 2014, **111**, 741–747.

253 S. Woo, C. H. Suh, S. Y. Kim, J. Y. Cho and S. H. Kim, Diagnostic performance of magnetic resonance imaging for the detection of bone metastasis in prostate cancer: a systematic review and meta-analysis, *Eur. Urol.*, 2018, **73**, 81–91.

254 I. Jardak, F. Hamza, Y. Hentati, W. Amouri, F. Kallel, M. Maaloul, S. Charfeddine, K. Chtourou, Z. Mnif and F. Guermazi, Place of SPECT/CT of the axial skeleton in the diagnosis of bone metastases: Prospective study about 150 cases, *Nucl. Med. Commun.*, 2018, **42**, 78–87.

255 J. G. Zhang, G. Z. Zhai, B. Yang and Z. H. Liu, Computerized tomography (CT) updates and challenges in diagnosis of bone metastases during prostate cancer, *Curr. Med. Imaging*, 2020, **16**, 565–571.

256 F. Kizilay, M. Sahin, A. Simsir, B. Turna, I. Cureklibatir and O. Omur, Predictive value of bone scintigraphy in the diagnosis of prostate cancer bone metastases and comparison of verification methods, *Kuwait Med. J.*, 2020, **52**, 368–374.

257 H. L. Yang, T. Liu, X. M. Wang, Y. Xu and S. M. Deng, Diagnosis of bone metastases: a meta-analysis comparing (1)(8)FDG PET, CT, MRI and bone scintigraphy, *Eur. Radiol.*, 2011, **21**, 2604–2617.

258 A. M. Aisen, W. Martel, E. M. Braunstein, K. I. Mcmillin, W. A. Phillips and T. F. Kling, MRI and CT evaluation of primary bone and soft-tissue tumors, *Am. J. Roentgenol.*, 1986, **146**, 749–756.

259 T. Hamaoka, J. E. Madewell, D. A. Podoloff, G. N. Hortobagyi and N. T. Ueno, Bone imaging in metastatic breast cancer, *J. Clin. Oncol.*, 2004, **22**, 2942–2953.

260 M. Stubbs, Application of magnetic resonance techniques for imaging tumour physiology, *Acta Oncol.*, 1999, **38**, 845–853.

261 I. Fogelman, G. Cook, O. Israel and H. Van, der Wall, Positron emission tomography and bone metastases, *Semin. Nucl. Med.*, 2005, **35**, 135–142.

262 J. Y. Choi, Treatment of bone metastasis with bone-targeting radiopharmaceuticals, *Nucl. Med. Mol. Imaging*, 2018, **52**, 200–207.

263 J. Goyal and E. S. Antonarakis, Bone-targeting radiopharmaceuticals for the treatment of prostate cancer with bone metastases, *Cancer Lett.*, 2012, **323**, 135–146.

264 Z. Y. Zhang, R. D. Ross and R. K. Roeder, Preparation of functionalized gold nanoparticles as a targeted X-ray contrast agent for damaged bone tissue, *Nanoscale*, 2010, **2**, 582–586.

265 Z. Z. Chen, H. C. Yu, W. Lu, J. K. Shen, Y. Wang and Y. Y. Wang, Bone-seeking albumin-nanomedicine for in vivo imaging and therapeutic monitoring, *ACS Biomater. Sci. Eng.*, 2020, **6**, 647–653.

266 S. W. Liu, L. Wang, M. Lin, Y. Liu, L. N. Zhang and H. Zhang, Tumor photothermal therapy employing photothermal inorganic nanoparticles/polymers nanocomposites, *Chin. J. Polym. Sci.*, 2019, **37**, 115–128.